agronomy

MDPI

Article

Multivariate Insight into Soil Organic Matter Dynamics in Subarctic Abandoned Farmland by the Chronosequence Approach

Timur Nizamutdinov [1,*], Sizhong Yang [2], Xiaodong Wu [2], Vladislav Gurzhiy [3] and Evgeny Abakumov [1]

[1] Department of Applied Ecology, Faculty of Biology, St. Petersburg State University, 7/9 Universitetskaya Nab., St. Petersburg 199034, Russia; e.abakumov@spbu.ru
[2] Cryosphere Research Station on the Qinghai–Tibet Plateau, State Key Laboratory of Cryospheric Science and Frozen Soil Engineering, Northwest Institute of Eco–Environment and Resources, Chinese Academy of Sciences, 320 Donggang West Road, Lanzhou 730000, China; yangsz@lzb.ac.cn (S.Y.); wuxd@lzb.ac.cn (X.W.)
[3] Department of Crystallography, Institute of Earth Sciences, St. Petersburg State University, 7/9 Universitetskaya Nab., St. Petersburg 199034, Russia; vladislav.gurzhiy@spbu.ru
* Correspondence: t.nizamutdinov@spbu.ru or timur_nizam@mail.ru

Abstract: Agricultural land abandonment is a widespread phenomenon found in many regions of the world. There are many studies on post-agricultural changes in temperate, arid, semi-arid regions, etc., but studies of such soils in boreal or Arctic conditions are rare. Our study aims to fill the gaps in research on the processes of post-agricultural soil transformation, with a focus on the harsh climatic conditions of the Arctic and Subarctic regions. Parameters of soil organic matter (SOM) are largely reflected in the quality of soil, and this study investigates the dynamics of SOM properties in Subarctic agricultural soils in process of post-agrogenic transformation and long-term fertilization. Using a chronosequence approach (0–25 years of abandonment) and a reference site with over 90 years of fertilization, we performed elemental (CHN-O) analysis, solid-state ^{13}C NMR spectroscopy of SOM, PXRD of soil and parent material, and multivariate statistical analysis to identify the connections between SOM composition and other soil properties. The results revealed transient increases in soil organic carbon (SOC) during early abandonment (5–10 years; 3.75–4.03%), followed by significant declines after 25 years (2.15–2.27%), driven by mineralization in quartz-dominated soils lacking reactive minerals for organo-mineral stabilization. The reference site (the Yamal Agricultural Station) maintained stable SOC (3.58–3.83%) through long-term organic inputs, compensating for poor mineralogical protection. ^{13}C NMR spectroscopy highlighted shifts from labile alkyl-C (40.88% in active fields) to oxidized O-alkyl-C (21.6% in late abandonment) and lignin-derived aryl-C (15.88% at middle abandonment), reflecting microbial processing and humification. Freeze–thaw cycles and quartz dominance mineralogy exacerbated SOM vulnerability, while fertilization sustained alkyl-C (39.61%) and balanced C:N (19–20) ratios. Principal Component Analysis linked SOC loss to declining nutrient retention and showed SOM to be reliant on physical occlusion and biochemical recalcitrance, both vulnerable to Subarctic freeze–thaw cycles that disrupt aggregates. These findings underscore the fragility of SOM in Subarctic agroecosystems, emphasizing the necessity of organic amendments to counteract limitations of poor mineralogical composition and climatic stress.

Keywords: Arctic; Yamal; fallow lands; agroecosystems; post-agricultural shifts; plaggic podzols; sandy soils; ^{13}C NMR; SOM; PXRD; soil minerals

Academic Editor: Cledimar Rogerio Lourenzi, Arcângelo Loss and Heike Knicker

Received: 28 February 2025
Revised: 28 March 2025
Accepted: 1 April 2025
Published: 3 April 2025

Citation: Nizamutdinov, T.; Yang, S.; Wu, X.; Gurzhiy, V.; Abakumov, E. Multivariate Insight into Soil Organic Matter Dynamics in Subarctic Abandoned Farmland by the Chronosequence Approach. *Agronomy* **2025**, *15*, 893. https://doi.org/10.3390/agronomy15040893

1. Introduction

The abandonment of agricultural land has emerged as a significant ecological and socioeconomic phenomenon observed across diverse global regions, with profound implications for ecosystem dynamics and carbon cycling [1,2]. Current estimates suggest that approximately 2.2 million km^2 of formerly cultivated land has been abandoned worldwide, representing nearly 1.5% of the Earth's terrestrial surface [3]. Notably, Russia accounts for roughly 25% of this total (with about 706,000 km^2 land having been abandoned)—a legacy of post-Soviet socioeconomic transitions and shifting agricultural priorities [3,4]. Following abandonment, these landscapes typically undergo secondary ecological succession, a process whereby vegetation gradually regenerates, often progressing toward a state resembling pre-agricultural ecosystems [5]. However, the trajectory and pace of recovery are highly variable, influenced by interactions between historical land use, regional climate, and biotic factors [6,7]. There are many studies on post-agricultural changes in soils [1,3,4,8,9] and several large meta-analyses and reviews on this topic [2,6,7,10–12], but only a few studies on post-agricultural ecosystems in Subarctic and Arctic environments [13–15].

Soil carbon sequestration following land-use change is a critical yet complex process shaped by a multitude of interdependent variables [16]. Climatic conditions, particularly temperature and precipitation regimes, exert a dominant influence by regulating both plant productivity—the primary source of soil organic matter—and microbial decomposition rates [16,17]. For instance, cooler, moisture-limited environments may favor slower decomposition and enhanced carbon storage, whereas warmer, humid regions often experience accelerated soil organic matter turnover [18]. Soil texture further modulates these dynamics, with fine-textured soils (e.g., clays) exhibiting greater carbon stabilization capacity due to mineral–organic associations compared to coarse-textured soils [19]. Additionally, site-specific factors, such as prior land management practices (e.g., tillage intensity and fertilizer use), vegetation composition during succession, and the duration since abandonment collectively determine the magnitude and direction of soil carbon changes [10,11]. Soil organic matter (SOM) is the major component of soils that is crucial for the functionality of agroecosystems [20]. It influences soil fertility, soil structure, and biological activity, and it contributes to resistance to erosion and climate change [21]. SOM also serves as a reliable indicator of soil quality, as its composition and structure are closely related to organic matter transformation processes that occur under the influence of anthropogenic activities and natural factors [22,23]. The investigation of SOM is of particular importance in Subarctic regions, which are characterized by low temperatures, short vegetation periods, and low rates of biogeochemical processes. Under such climatic conditions, anthropogenic impacts, including intensive agricultural use, can lead to significant changes in the SOM system [24–26]. Analysis of these changes has particular relevance for assessing land-use implications and developing strategies and perspectives for the development of local agriculture and improvement of food security in the northern regions [27–29].

The Subarctic climate zone, characterized by permafrost-affected soils and extreme seasonal variability, presents unique challenges and opportunities for agricultural land use and SOM dynamics [30,31]. In regions such as the Yamal (Yamal–Nenets Autonomous District), the legacy of Soviet-era, agricultural expansion has left a mosaic of active and abandoned cropland and farmlands [32,33]. These landscapes serve as critical case studies for understanding how SOM systems evolve under anthropogenic disturbance and subsequent natural recovery, particularly in cryogenic ecosystems where soil processes are tightly coupled with temperature dynamics. The Yamal region's agricultural soils also face unique climatic pressures. Rising Arctic temperatures are projected to deepen the active layer, potentially accelerating SOM mineralization and greenhouse gas emissions [22,34]. Alternatively, the region's abandoned lands may act as unexpected carbon sinks, if veg-

etative recovery and microbial adaptation offset these losses, or could be re-involved in agricultural practices [25,35]. Commonly, land abandonment has been linked to increased soil aggregation and carbon sequestration, driven by the recovery of plant-root systems and microbial necromass accumulation [12]. In Arctic and Subarctic zones, these processes are further influenced by permafrost thaw and active-layer dynamics, which influence soil moisture regimes and SOM stabilization pathways [36]. It has previously been shown that microbial communities in abandoned Yamal soils exhibit distinct taxonomic profiles compared to undisturbed tundra, with reduced diversity in anthropogenically disturbed sites, potentially slowing SOM turnover [37]. Usually, the physical protection of SOM within aggregates—a key mechanism for carbon storage in temperate regions—may be less effective in permafrost-affected soils due to cryogenic mass transfer (freeze–thaw cycles) disrupting aggregate stability [38,39]. Agricultural activities in different environmental conditions have a specific impact on the molecular and elemental composition of SOM [40,41]. It can be assumed that the discontinuation of agricultural activity is accompanied by a slow recovery of the SOM structure; the stabilization of SOM and accumulation of aromatic compounds occur against the background of a general increase in the resistance of organic matter to decomposition. These processes can take decades and are associated with extreme climatic conditions and a short growing season [42,43]. The intensity and direction of these changes depend on climatic conditions, agrotechnologies, and the duration of land use [44]. Investigation of these processes in abandoned and active agricultural soils of the Subarctic and Arctic will reveal the long-term consequences of the economic activity of humankind, as well as assess the potential of ecosystem functions of agrogenically transformed soils.

^{13}C NMR spectroscopy is a widely used tool for SOM analysis. This method allows a detailed characterization of the composition of SOM, including the distribution of various functional groups, such as aromatic, aliphatic, and carboxylic compounds [45]. ^{13}C NMR provides information on the ratio of stable and labile fractions of SOM, which is key to understanding the stability of organic matter and its resistance to degradation [46]. The agricultural management practices examined in this study altered the stability of SOM by modifying the distribution of its carbon functional groups. Specifically, these practices shifted the relative abundance of alkyl, O-alkyl, aromatic, and carbonyl carbon groups within SOM. Fertilizer use, implemented to boost crop productivity, was found to elevate the proportion of O-alkyl carbon functional groups [47]. The combined application of ^{13}C NMR and elemental analysis provides a comprehensive assessment of changes in the SOM system, combining structural detail and quantitative parameters, which is particularly important in anthropogenically disturbed soils, as agricultural practices (fertilizer application and tillage) alter both the elemental composition and structural diversity of SOM [48,49].

Earlier [13], we obtained data that showed that in the soils of the chronosequence of abandoned farmlands (0–5–10–16–17–20–25 years old) in the vicinity of Salekhard, there was a decrease in the SOC/clay ratio (r^2 = 0.95), which indirectly indicates the degradation of soil structure, and we made an assumption that these soils are not able to stabilize the carbon pool over this long period of time. To verify this hypothesis, we put forward a number of objectives: I—To characterize temporal shifts in SOM composition and stability in a post-agricultural chronosequence (0–25 years) using elemental analysis and ^{13}C NMR spectroscopy to identify biochemical and structural changes. II—To compare SOM dynamics between abandoned soils and a long-term fertilized reference site to assess the effectiveness of organic additives in mitigating SOM loss under Subarctic conditions. III—To identify key factors for SOM stability using multivariate statistics (PCA) linking basic soil properties (pH, C:N ratio, DOC, etc.) and SOM quality management practices.

2. Materials and Methods

A chronosequence analysis was applied to study agricultural soils with varying durations of abandonment in the Yamal–Nenets Autonomous District, Russia, near Salekhard. This region lies within the permafrost zone, close to the Arctic Circle (66°30′ N, 66°42′ E), at the southern edge of the forest–tundra ecotone. Characterized by a Subarctic climate (Köppen classification: Dfc), the area experiences a mean annual air temperature of −5.1 °C, with extremes averaging −23.1 °C in January and +15 °C in July. Sub-zero temperatures persist for up to 240 days annually, while the growing season lasts fewer than 70 days. Precipitation averages approximately 500 mm per year, peaking markedly during summer months [50]. The investigated abandoned and active agricultural fields (Table 1) are located on the high right bank of the Ob River. A detailed map with the sampling location can be found in paper [13]; the coordinates of the sampling locations are given in Table 1. By analyzing archival satellite images and interviewing the local population, it was established that these plots were actively used for growing various cultures in the 1970s and 1980s and belonged to the Yamal experimental agricultural station (YAS) [51].

Table 1. Classification of soils, degree of abandonment for each field, and sampling coordinates.

Sample Code								
S5	S6	S8	S4	S2	S3	S1	S10	S11
Soil according to WRB 2022 [52]								
Hortic Podzol (Arenic, Cordic)	Plaggic Albic Podzol (Arenic, Cordic)	Plaggic Ortsteinic Podzol (Arenic)	Plaggic Turbic Gleyic Ortsteinic Podzol (Arenic)	Plaggic Turbic Ortsteinic Podzol (Siltic)	Plaggic Podzol (Siltic, Cordic)	Plaggic Ortsteinic Podzol (Siltic)	Plaggic Podzol (Turbic)	Histic Entic Podzol (Folic)
Age of abandonment								
0	5	10	16	17	20	25	YAS *	Mature
Sampling site coordinates (WGS 84)								
N66.5067° E66.6920°	N66.5069° E66.6984°	N66.5132° E66.6938°	N66.5030° E66.7004°	N66.5016° E66.6976°	N66.5020° E66.6912°	N66.4977° E66.6911°	N66.5266° E66.6552°	N66.5169° E66.6967°

*—Yamal Agricultural Station.

The fieldwork was conducted in August 2023. According to interviews with local people, the main crops in these fields have always been potatoes and forage plants for livestock fodder. The soil sampling strategy was as follows: at each of the sites (Table 1), a full soil section was made, and, additionally, 3 sampling points from topsoil (plow/post-plow) horizons were established. For this study, samples were taken from the 5–15 cm layer. A total of 4 separate sub-samples from the 5–15 cm layer were obtained for each field, from which an average sample was then formed. Before preparing the average sample, each sub-sample was air-dried at room temperature (24–25 °C) and sieved through a 1 mm mesh sieve. The average sample was then prepared by mixing equal proportions of the 4 previously prepared sub-samples.

Before elemental analysis and ^{13}C NMR spectroscopy, the soil samples were purified. To remove paramagnetic minerals (e.g., Fe^{3+} and Mn^{2+}) that may interfere with NMR signals and concentrate SOM, the samples were demineralized with 10% (*v*/*v*) hydrofluoric acid (HF) prior to NMR analysis. We used a modification of procedures from [53,54]. The following is a brief description of the procedure: (1) A quantity of 15.0 ± 0.5 g of soil (air-dried and sieved through a 1 mm mesh sieve) was placed in a high-speed centrifuge

tube (50 mL). (2) Then, 30 mL of 10% HF was added to each centrifuge tube. (3) The tubes with soil were placed on an orbital rotator and shaken for 8 h and then centrifuged (6000 rpm, 30 min). (4) Following the centrifugation step, the supernatant was discarded. The HF treatment procedure was repeated a further five times for each sample. (5) After the final HF treatment, the samples were washed with distilled water (the procedure was similar to the HF treatment), and the degree of purification was assessed by the pH value of the supernatant. If the pH of the supernatant was less than 6.5–7, the washing was continued (as a rule, 3–4 water treatments were sufficient to clean the sample of HF). (6) After cleaning, the samples were oven-dried at 65 °C and gently ground and homogenized using an agate mortar and pestle.

The elemental composition of the samples was determined using an elemental CHN-analyzer (Euro EA 3028-HT; EuroVector Instruments & Software, Milan, Italy); the procedure performed in triplicate. The results of the elemental analysis of the demineralized samples were re-calculated, taking into account the ash contents. Ash content (Table 2) was determined by the gravimetric method by ignition of the sample at 550 °C for 8 h (before ash content determination and elemental analysis, the samples were dried at 105 °C to a constant weight to remove moisture). The O content (%) was determined by the difference—100 − (N, % + C, % + H, %). O:C, C:N, and H:C ratios were determined on the basis of atomic percents.

Table 2. Ash contents in demineralized and dried soil samples.

Demineralized Sample (n = 3)								
S5	S6	S8	S4	S2	S3	S1	S10	S11
Ash, % (mean ± SD)								
34.5 ± 0.4	22.1 ± 0.8	33.8 ± 0.0	31.6 ± 0.1	28.1 ± 0.5	27.7 ± 0.8	41.9 ± 0.1	29.3 ± 0.0	0.8 ± 0.1

Solid-state CP/MAS ^{13}C NMR spectra of concentrated SOM separated from soils were measured with a Bruker Avance 500 NMR spectrometer (Bruker BioSpin GmbH, Rheinstetten, Germany) in a 3.2 mm ZrO_2 rotor. The magic-angle spinning frequency was 20 kHz in all cases, and the nutation frequency for cross-polarization was u1/2p 1/4 62.5 kHz. The repetition delays were 3 s. The number of scans was 6500–32,000. The contact time was 0.2 µs. The spectra were quantified by subdividing them into the following chemical shift regions: 0–45 ppm (alkyl), 45–60 ppm (N-alkyl and methoxyl), 60–110 ppm (O-alkyl), 110–140 ppm (aryl), 140–160 ppm (O-aryl), 160–190 ppm (carboxyl), and 190–230 ppm (carbonyl) [44]. The ^{13}C intensity distribution was determined by integrating the signal intensity over the shift regions of the chemicals using MestReNova 12.0 software (Mestrelab Research, Santiago de Compostela, Spain).

For each sample of SOM, the relative intensity of each band and integral indexes—(Equations (1)–(3)): aromaticity index (ARM), hydrophobicity index (HB/HI), and alkyl C/O-alkyl C (A/OA) ratio—were calculated based on the respective chemical shifts [44,55].

$$ARM = \frac{Area\ (110–160\ \text{ppm})}{Area\ (0–160\ \text{ppm})} \quad (1)$$

$$\frac{HB}{HI} = \frac{Area\ (0–45\ \text{ppm}) + Area\ (110–160\ \text{ppm})}{Area\ (45–110) + Area\ (160–220\ \text{ppm})} \quad (2)$$

$$\frac{A}{AO} = \frac{Area\ (0–45\ \text{ppm})}{Area\ (45–110\ \text{ppm})} \quad (3)$$

The determination of the carbon contents of the dissolved organic compounds (DOCs) was carried out in an aqueous extract from bulk soil samples. Three soil subsamples weighing about 10 g from each sample of bulk soil were filled with 25 mL of distilled water, shaken on a rotator for 15 min and left for 24 h, then shaken for an additional 15 min [56]. The suspension was filtered through a paper filter, and the volume of filtrate was registered. Further, the DOC content was determined according to the Walkley–Black method (colorimetric modification) [57], but instead of a soil sample, 10 mL of filtrate of aqueous extract was taken. The results obtained for the carbon contents in the aliquots were converted to the DOC contents for the soil samples and to the percentages of DOC contents from the total organic carbon content in the soil [56].

To determine the mineralogical composition of the bulk soil samples from the Yamal experimental agricultural station, they were ground in an agate mortar for in situ examination using a Rigaku MiniFlex II powder X-ray diffractometer (PXRD; Rigaku Corporation, Tokyo, Japan) equipped with a 1D silicon strip PSD D/teX Ultra detector operated with CoKα radiation at 30 kV and 15 mA in a Bragg–Brentano geometry. PXRD data were collected in the range of 3–80° 2θ. Phase identification was carried out using the ICDD PDF-2 Database (released 2022).

Cation exchange capacity (CEC, mEq/100 g) was measured in bulk soil samples using the Bobko–Askinazi–Aleshin method [58]. Briefly, $BaCl_2$ buffer solution (pH = 6.5) was poured over a sample of soil (2–3 g), and saturation of the soil was carried out on paper filters until the volume of the filtrate was equal to 150–200 cm^3. After saturation, the paper filters with the soil were dried and transferred to a glass, then 100 cm^3 of H_2SO_4 solution (0.05 N) was poured over them. After that, the suspensions were filtered, and 20 cm^3 aliquots were taken from the filtrate and titrated with NaOH solution (0.1 N). Then, the value of the CEC was calculated according to Equation (4).

$$CEC = \frac{(V - V1) \times C \times V2 \times 100}{V3 \times m} \quad (4)$$

where V is the volume of NaOH solution, consumed for control titration of 20 cm^3 of pure H_2SO_4, cm^3; V1 is the volume of NaOH solution, consumed for titration of 20 cm^3 of filtrate, obtained by displacement of Ba^{2+} with H_2SO_4, cm^3; C is the molar concentration of NaOH solution, mol dm^{-3}; V2 is the volume of H_2SO_4 taken for displacement of Ba absorbed by soil, cm^3; m is the mass of the air-dried soil sample, g; V3 is the volume of filtrate taken for titration, cm^3; and 100 is the conversion factor per 100 g of soil.

We also used some soil physical parameters that were obtained in the previous study; briefly, these parameters changed from S5 to S1 as follows: bulk density (g cm^{-3})—1.1 to 1.3 (r^2 = 0.05), clay (%)—5.3 to 12.4 (r^2 = 0.84), silt + clay (%)—11.2 to 20.2 (r^2 = 0.89), and SOC/clay—0.52 to 0.18 (r^2 = 0.95). A detailed description of these soil parameters is given in our previous work [13] and in Appendix A.

The Principal Component Analysis (PCA) method was chosen for multivariate data analysis. For PCA analysis, a data matrix was compiled from previously published data and data obtained in this study. The total matrix consisted of 16 variables: bulk density, pH in water suspensions, SOC and TN in bulk soil, C:N ratio, clay in bulk soil, concentrations of N minerals (NH_4 and NO_3) in bulk soil, and available P and K, which were taken from our previous study [13] (Appendix A, Table A1). The DOC and the O:C, C:N, and H:C ratios in SOM, as well as A/O-A and HB/HI values in SOM and the degree of aromaticity (ARM), were taken for PCA from this study. The suitability of the data for PCA was determined by performing Kaiser–Meyer–Olkin (KMO) and Bartlett tests, using IBM SPSS Statistics (Version 27.0), according to the methodology described in [59,60]. Further PCA was then performed using Origin (Pro) (Version 2024; OriginLab Corporation, Northampton, MA,

USA), using the Kaiser rule (data were previously subjected to Z-score normalization). We used orthogonal rotation of the data matrix using the Varimax method; variables with loadings above |0.6| were considered significant.

Further statistical processing and visualization of data were carried out using GraphPad Prism version 10.2.3 (GraphPad Software, Boston, MA, USA) and Origin (Pro) (Version 2024; OriginLab Corporation, Northampton, MA, USA).

3. Results

The SOM elemental analysis data (Figure 1) show that for the chronoseries of the soils (S1–S8), the contents of major elements had the following values (means ± SDs, n = 21): C—47.82 ± 2.69%, CV = 0.05; N—1.87 ± 0.28%, CV = 0.15; H—6.64 ± 0.44%, CV = 0.06; O—43.66 ± 2.54%, CV = 0.06.

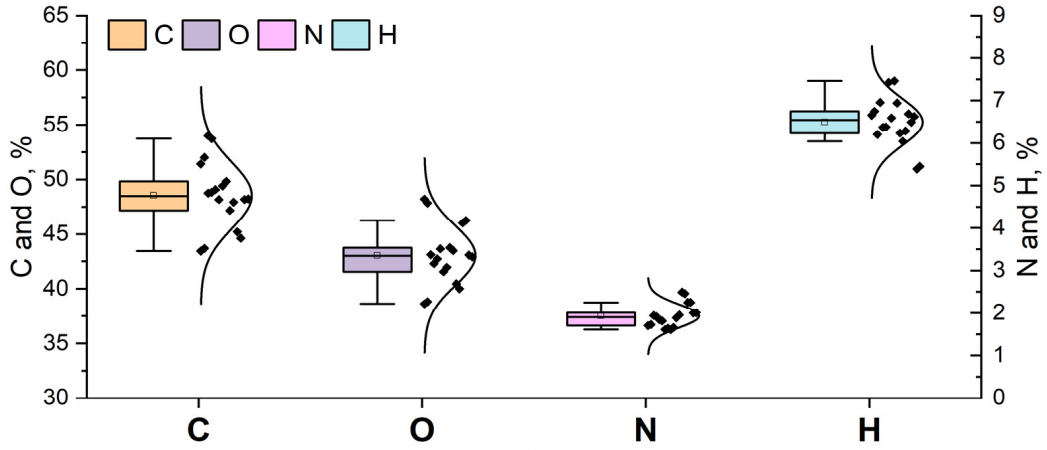

Figure 1. Box chart with normal distribution curve of variations in C, N, H, and O contents in SOM (mass %).

In actively cultivated soils (S5, 0 years abandoned), SOM is characterized by a relatively high C content (47.55 ± 0.53%, n = 3) and a moderate N concentration (1.63 ± 0.03%, n = 3), indicative of fresh organic inputs from agricultural activity. The H content remains stable at 7.20 ± 0.37% (n = 3), while O is around 43.62 ± 0.20% (n = 3) of SOM. After five years of abandonment (S6), a noticeable increase in the SOM C content (51.72 ± 0.41%, n = 3) and N content (1.92 ± 0.05%, n = 3) can be observed, while the O percentages decrease to 40.23 ± 0.32% (n = 3). The H content slightly declines to around 6.14 ± 0.14% (n = 3). By the tenth year of abandonment (S8), the N content rises significantly (2.48 ± 0.02%, n = 3), and the SOM C content declines to 44.91 ± 0.42% (n = 3). The O increases to 46.13 ± 0.16%, and the H levels remain relatively stable at 6.48 ± 0.28%. In later abandonment stages (16–20 years; S4, S2, and S3), the C content is 48.16–49.82%, with N concentrations of 1.61–1.94%. O levels are between 41.55% and 43.65%, while the H content is within the 6.20–7.42% range. After 25 years of abandonment (S1), the N content slightly declines (1.71 ± 0.02%, n = 3), while C levels drop notably to 43.56 ± 0.17%. The O fraction increases to 48.02 ± 0.25% (n = 3), and H remains relatively stable (6.70 ± 0.06%, n = 3). In comparison, the field at the Yamal Agricultural Station (S10) maintains a moderate SOM composition, with C levels of 48.20 ± 0.04%, N at 2.25 ± 0.00%, and O at 42.99 ± 0.14% (mean ± SD, n = 3). The mature Histic Podzol (S11) exhibits the highest SOM C content (53.86 ± 0.18%, n = 3) and the lowest H (5.42 ± 0.04%, n = 3) and O levels (38.72 ± 0.13%, n = 3), reflecting highly decomposed, well-humified organic matter typical of natural peat-accumulating soils [61].

The data (Figure 2) were derived from ^{13}C NMR spectroscopy, which quantifies the relative abundance of carbon types in SOM based on their chemical shift regions. Key functional groups include alkyl C (0–45 ppm), N-alkyl and methoxyl C (45–60 ppm), O-alkyl C (60–110 ppm), aryl C (110–140 ppm), O-aryl C (140–160 ppm), carboxy C (160–190 ppm), and carbonyl C (190–220 ppm) [27,45]. General statistics for the SOM molecular composition in the soil chronosequence are as follows (n = 7, means ± SDs): alcyl C—36.78 ± 3.41%, CV = 9.03; N-alkyl and methoxyl C—6.04 ± 0.67%, CV = 11.16; O-alkyl C—21.87 ± 2.35%, CV = 10.76; aryl C—13.57 ± 1.57%, CV = 11.55; O-aryl C—6.56 ± 0.83%, CV = 12.59; carboxy C—11.72 ± 0.74%, CV = 6.28; carbonyl C—3.51 ± 0.59%, CV = 16.73. A detailed distribution of the molecular composition of the SOM is given below and in Table 3.

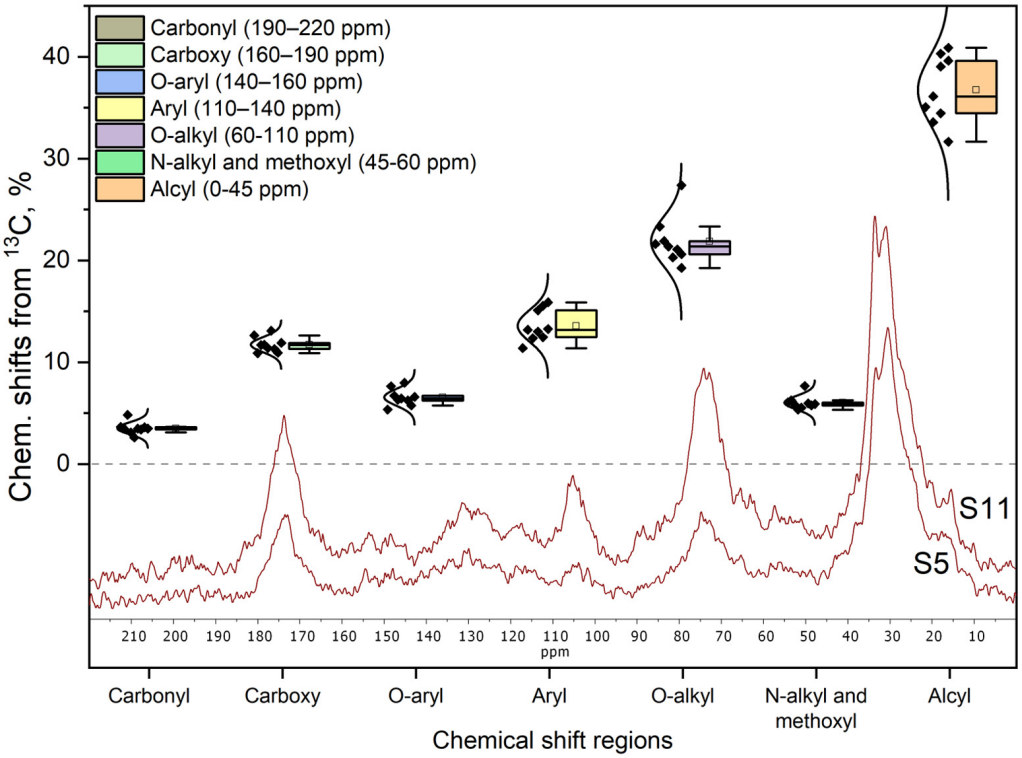

Figure 2. Box chart with normal distribution curve—relative abundance of the different functional groups obtained by the integration of the peaks area from the ^{13}C NMR results. S11 and S5—representable ^{13}C solid-state nuclear magnetic resonance spectra (^{13}C NMR) of the concentrated SOM samples for mature soil (S11) and soil of cultivated fields (S5).

Active Agricultural Field (S5, 0 Years of Abandonment): alkyl C (0–45 ppm)—40.88%; N-alkyl and methoxyl C (45–60 ppm)—5.75%; O-alkyl C (60–110 ppm)—20.61%; aryl C (110–140 ppm)—12.45%; O-aryl C (140–160 ppm)—5.75%; carboxyl C (160–190 ppm)—10.93%; carbonyl C (190–220 ppm)—3.61%. Early Abandonment (S6, 5 Years): alkyl C—39.04%; O-alkyl C—21.08%; aryl C—13.00%; carboxyl C—11.30%. Mid-Abandonment (S8, 10 Years): alkyl C—31.65%; aryl C—15.88%; O-aryl C—7.97%; carboxyl C—13.08%.

Late Abandonment (S1, 25 Years): alkyl C—35.06%; N-alkyl and methoxyl C—6.25%; O-alkyl C—21.59%; aryl C—15.09%; O-aryl C—7.63%; carboxyl C—10.88%; carbonyl C—3.47%. SOM of the field at the Yamal Agricultural Station (S10): alkyl C—39.61%; N-alkyl and methoxyl C—5.90%; O-alkyl C—19.26%; aryl C—13.26%; O-aryl C—6.60%; carboxyl C—11.89%; carbonyl C—3.48%. SOM of undisturbed peat soil (S11, Histic Podzol): alkyl C—33.56%; N-alkyl and methoxyl C—6.05%; O-alkyl C—27.37%; aryl C—11.38%; O-aryl C—5.36%; carboxyl C—12.64%; carbonyl C—3.64%.

For recently abandoned agricultural soils (S5–S1, 0–25 years), the DOC content (Figure 3) varies between 0.01% and 0.08%, with a general tendency to range between 0.02% and 0.06% across different abandonment periods. The proportion of DOC relative to SOC is relatively low, spanning from 0.000302 to 0.002112%. The reference site, S10 (Yamal Agricultural Station), exhibits DOC values similar to the younger abandoned sites, ranging from 0.03% to 0.04%, with DOC as a percentage of SOC between 0.000939 and 0.001708%. In contrast, the undisturbed peat soil (S11) shows significantly higher DOC values, ranging from 0.30% to 0.43%. The DOC as a percentage of SOC in this site is notably higher (0.098594–0.139221%).

Table 3. The ^{13}C intensity distribution determined by integrating the signal intensity (YAS—Yamal Agricultural Station, MT—mature peat soil).

Sample	Age	Functional Groups of C							Integral Indexes		
		Alcyl	N-alkyl	O-alkyl	Aryl	O-aryl	Carboxyl	Carbonyl			
		Chemical Shifts from ^{13}C, %							ARM	HB/HI	A/A-O
		0–45	45–60	60–110	110–140	140–160	160–190	190–220			
S5	0	40.88	5.75	20.61	12.45	5.75	10.93	3.61	0.21	1.44	1.55
S6	5	39.04	5.96	21.08	13.00	6.23	11.30	3.39	0.23	1.40	1.44
S8	10	31.65	7.67	20.28	15.88	7.97	13.08	3.47	0.29	1.25	1.13
S4	16	40.31	5.52	21.37	12.35	6.45	11.40	2.60	0.22	1.45	1.50
S2	17	36.10	5.33	21.89	15.54	6.32	11.72	3.10	0.26	1.38	1.33
S3	20	34.44	5.85	23.33	13.18	6.70	11.68	4.82	0.24	1.19	1.18
S1	25	35.06	6.25	21.60	15.09	7.64	10.88	3.48	0.27	1.37	1.26
S10	YAS	39.61	5.90	19.26	13.26	6.60	11.89	3.48	0.23	1.47	1.57
S11	MT	33.56	6.05	27.37	11.38	5.36	12.64	3.64	0.20	1.01	1.00
Mean		36.74	6.03	21.87	13.57	6.56	11.72	3.51	0.24	1.33	1.33
SD		3.32	0.67	2.35	1.57	0.83	0.74	0.59	0.03	0.15	0.20
CV		9.03%	11.16%	10.76%	11.55%	12.59%	6.28%	16.73%	12.28%	11.40%	15.13%

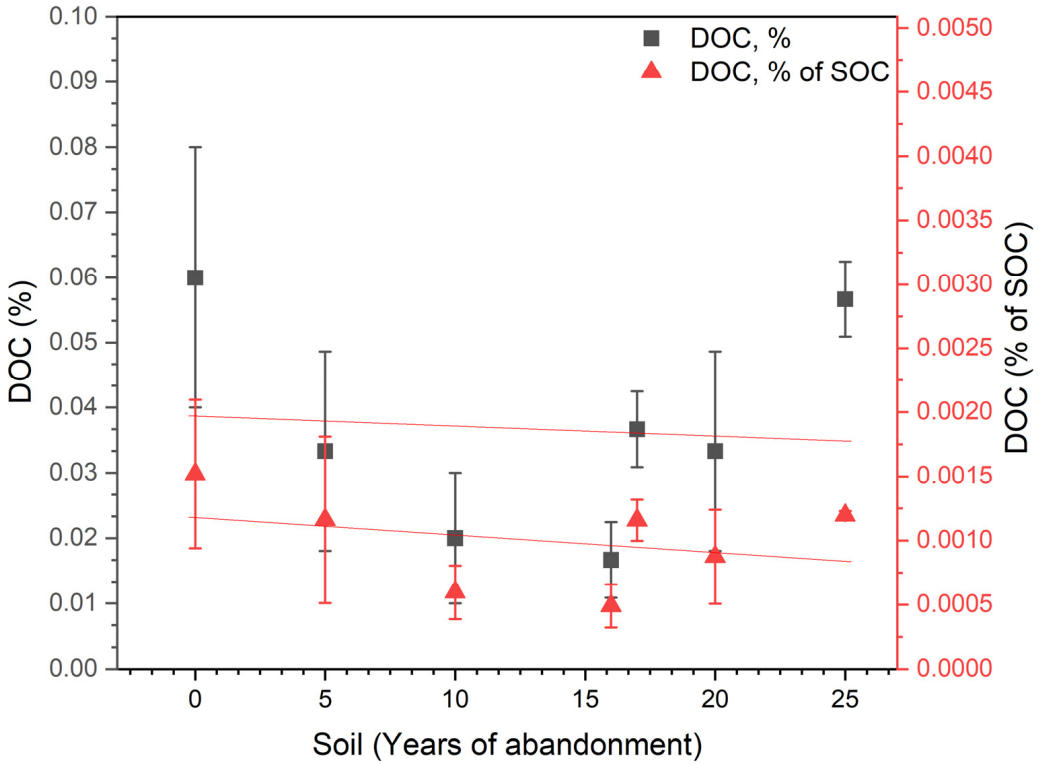

Figure 3. Dynamics of dissolved (DOC) organic carbon (mean ± SD, n = 3) change (in % of soil mass and in % of soil organic C) as a function of abandonment time.

The data matrix (16 variables), including pH, SOC, TN, C:N, clay, P, K, N-NH_4, and N-NO_3—from [13,31]—and DOC, SOM O:C, SOM C:N, SOM H:C, A/O-A, HB/HI, and ARM, were analyzed by principal component (PCA) analysis; data from sample S11—reference peat soil—were not included in the data matrix. Before PCA, we performed Kaiser–Meyer–Olkin (KMO) and Bartlett tests. KMO = 0.65 (mediocre sampling adequacy). Bartlett's test of sphericity: χ^2 = 394.8; *p*-value: < 0.001. These values confirmed the suitability of the data for PCA analysis. The data were normalized (Z-score standardization applied). For PCA analysis, Kaiser's rule was used—components with an eigenvalue > 1 were selected. Three significant components were selected: eigenvalues > 1, cumulative variance of ~76.5% (PC1—35.5%; PC2—25.9%; PC3—18.1%). Rotation of the matrix by the Varimax method was used. Significant variables within a component were selected with loadings above |0.6|. Table 4 shows the component loadings (Varimax-rotated) for selected variables. Figure 4 shows a biplot of the PCA analysis for selected data.

Table 4. Component loadings (Varimax-rotated). Key variables (|loadings| > 0.6) bolded.

Var.	Bulk Soil									SOM					
	pH	SOC	DOC	C:N	Clay	P	K	NH_4	NO_3	O:C	C:N	H:C	A/O-A	HB/HI	ARM
PC1	0.03	−0.34	**0.62**	**−0.84**	−0.24	**0.65**	**0.91**	**0.90**	0.41	0.31	0.16	0.55	0.42	0.40	−0.29
PC2	−0.03	**0.79**	−0.12	−0.01	−0.02	0.16	0.15	0.15	**0.70**	**−0.86**	0.31	**−0.72**	**0.83**	**0.63**	**−0.76**
PC3	**0.73**	0.38	−0.17	−0.42	0.35	**0.63**	−0.20	−0.23	0.48	0.28	**−0.91**	0.15	−0.10	−0.09	0.48

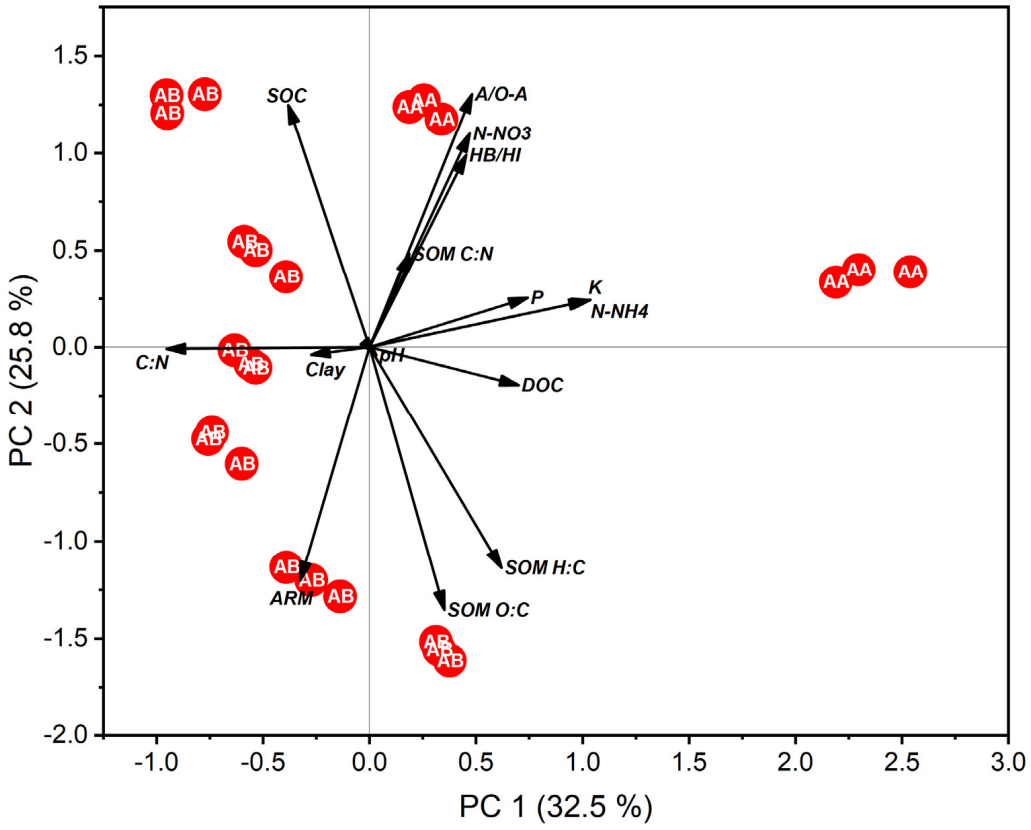

Figure 4. PCA Biplot for PC1 and PC2. AA—active agriculture (S5 and S10 samples), AB—abandoned fields (S6, S8, S4, S2, and S1 samples).

The PXRD data analysis from the Yamal Agricultural Station (Figure 5) soils reveal a mineralogical composition dominated by quartz, with significant contributions from vermiculite and Na and K feldspars (albite and orthoclase, respectively) and minor amounts of phlogopite and unidentified phases (with peak observed intensities below 1) in the plow

soil horizon (Figure 5A). Quartz (SiO_2)—key peaks: 2θ = 20.78° (d = 4.26 Å, observed intensity = 19), 2θ = 26.58° (d = 3.35 Å, observed intensity = 100—strongest peak); additional peaks at 36.52°, 50.10°, and 59.90° confirm its prevalence. Vermiculite (clay mineral)—key peaks: basal reflections at 2θ = 6.10° (d = 14.48 Å, (002)) and higher-order peaks (e.g., 12.43°, 18.72°), multiple overlapping peaks with feldspars and micas. Feldspars—albite ($NaAlSi_3O_8$), peaks at 27.88° (d = 3.20 Å) and other angles; orthoclase ($KAlSi_3O_8$), peaks at 27.43° (d = 3.25 Å) and other angles.

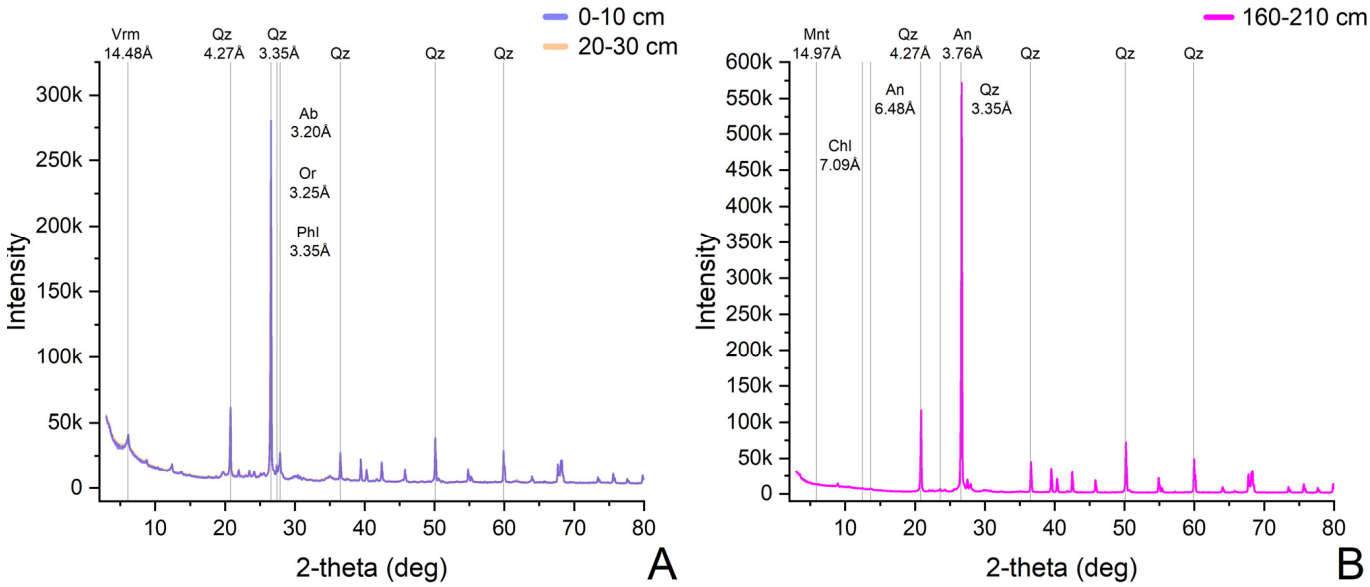

Figure 5. X-ray diffraction patterns of bulk soil samples from Yamal experimental agricultural station: (**A**) from plow horizon, from 0–10 cm—upper boundary and lower boundary of 20–30 cm plow horizon; (**B**) parent material from 160–210 cm depth. Vrm—vermiculite, Qz—quartz, Ab—albite, Or—orthoclase, Phl—phlogopite, Mnt—montmorillonite, An—anorthite, Chl—chlorite.

The dominant phases in the parent material (Figure 5B) were quartz, montmorillonite, anorthite, biotite, and some members of the chlorite–serpentine mineral group. Quartz was still a major component—2θ = 26.62° (d = 3.34 Å, observed intensity = 100.00). Additional peaks at 20.81, 36.56°, 50.15°, and 59.93° (similar to the topsoil) were observed. Montmorillonite (smectite clay)—key peaks: basal reflections at 2θ = 5.90° (d = 14.97 Å) and 26.66° (overlaps with quartz). Anorthite ($CaAl_2Si_2O_8$)—key peaks: 2θ = 13.63°, 23.57°, and 30.10° (d = 6.48–2.96 Å). Biotite ($K(Mg,Fe)_3AlSi_3O_{10}(OH)_2$)—key peaks—scattered peaks (e.g., 30.80° and 35.10°). Chlorite–serpentine group minerals—key peaks: 2θ = 5.90° and 12.46° (d = 14.97 and 7.09 Å, respectively).

Additionally, the cation exchange capacity (CEC) was measured in the soil of the Yamal experimental agrostation and the soil chronosequence (Table 1). For the soils of the Yamal experimental agrostation, CEC = 12.97 ± 0.83 mEg/100 g (n = 3); this value was predominantly low but consistent with the mineralogical composition data (Figure 5). For soils from the chronoseries, a gradual decrease in CEC was observed, with a maximum in young fallow fields (Figure 6). For the soil in the active potato field (S5), CEC = 12.32 ± 0.68 mEg/100 g (n = 3); these values were close to those of the soil of the Yamal experimental station. The minimum CEC values were found in the soil of the oldest fallow field, which was more than 25 years old (S1)—9.47 ± 1.97 mEg/100 g (n = 3).

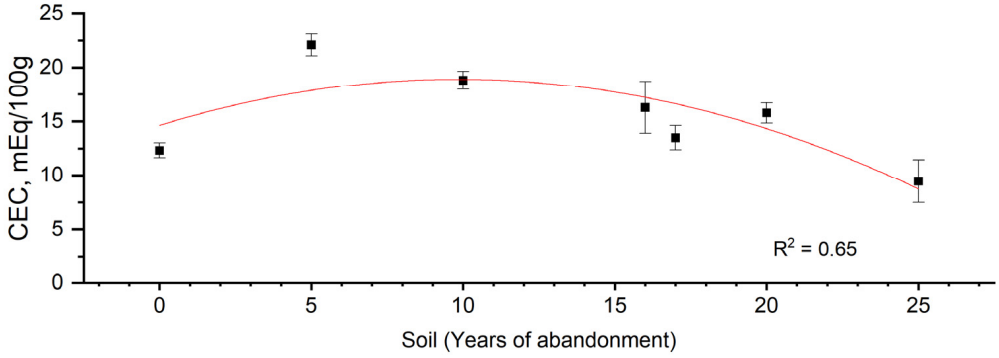

Figure 6. Cation exchange capacity (CEC, mEq/100 g) dynamics in agricultural soils with different fallow ages (mean ± SD, n = 3).

4. Discussion

Changes in SOM parameters in soils of abandoned lands vary across different regions, e.g., in Central Perineae, on lands abandoned since the 1950s, there was an increase in the contents and reserves of SOC and N at the primary stages of succession, and the SOM composition lacked lignin and was dominated by fatty acids [62]. In a semi-arid climate, in calcareous soils of the Central Zagros Mountains, SOC (7.0 Mg C ha^{-1}) accumulation occurred in the 0–30 cm layer on lands abandoned 18–22 years ago [63]. In the forest–steppe zone of Eastern Siberia, accumulation of 0.85 Mg C ha^{-1} in the 0–30 cm layer was shown in Haplic Luvisol. In abandoned croplands that were 0–7–25–60 years old, the main role in C sequestration was played by the mineral-associated pool of SOM, and labile fractions accumulated 2.8 times faster than stable ones [64]. In temperate, broad-leaved forest areas of European Russia, post-agricultural dynamics of SOM pools were linked to carbon accumulation within both active and passive pools [4]. Overall, it can be summarized that researchers generally agree that three key factors influence carbon pools in abandoned lands: climate, vegetation, and physical protection (aggregate stability) of SOM [65–68]. For our study, we had unique conditions that had not previously been investigated in terms of SOM in soils of post-agricultural agroecosystems—a Subarctic climate, secondary succession of forest tundra vegetation [13], and soils with a poor mineralogical composition (Figure 5). In addition, this study is distinguished by the fact that soil plowing was not carried out in situ, and soils for agricultural lands were pre-prepared [13].

We should first discuss general soil and SOM parameters of the Yamal experimental agrostation: long-term tillage (>90 years) with organic (peat and manure) and mineral fertilizers maintained the quantity and quality of SOM in the Yamal experimental field. Despite the Arctic conditions, the soil retains 3.6% SOC with a balanced molecular composition dominated by C alkyls (39.6%) and moderate aromaticity (0.23). Despite the dominance of quartz in the mineralogical composition and a small amount of clay (layered) minerals (Figure 5A), it is possible for organo-mineral interactions to form strong complexes with SOM, preserving alkyl C (microbial lipids) and reducing decomposition [49,69]. Continuous application of organic fertilizer (peat and manure) provides labile C (O-alkyl) and nitrogen (N), keeping the soil C:N (19–20) and C:N ratios in SOM (~25) low, which supports microbial activity [70]. Moderate bulk density (1.27 g cm^{-3}) and clay contents (13–15%) favor aggregate formation, physically protecting SOM from microbial access [71,72]. Other studies have shown that to maintain a stable amount of SOM in the soil of the Yamal Agricultural Station, peat should be applied to the soil every 6 years at a dose of 4 kg m^{-2} [73]. These findings are consistent with studies of temperate agricultural systems, where clay minerals and organic matter cooperatively stabilize SOM [74,75]. However, the Arctic context creates unique constraints, as cold temperatures slow microbial turnover, increasing the role of mineral defense [27]. High SOC (32.8%) and TN (1.48%) characterize Histic Entic

Podzol (S11), peat from which is used to fertilize agricultural fields. The peat contributes labile O-alkyl C (27.4%) but limited N, resulting in high C:N ratios in SOM (~31) and low aromaticity (0.20). Pure peat lacks mineral matrices for stabilization, making it vulnerable to oxidation during drainage [76]. However, when applied to relatively mineral-rich soils (S10), peat-derived carbon binds to the mineral matrix, increasing SOM stability [75].

Active fields (S5: 0 years) exhibit (Figure 7) moderate SOC (2.68–2.80%), while short-term abandonment (S6: 5 years) shows a spike (3.75–4.03%), likely due to reduced tillage and initial plant-residue accumulation. Older abandoned sites (S1: 25 years) display lower SOC values (~2.15–2.27%), suggesting progressive SOM mineralization [13]. Against the background of quartz dominance in the mineralogical composition, the small amount of layered minerals in soils and parent materials (Figure 5), and the decrease in the SOC/clay ratio (0.52 in S5 → 0.18 in S1), we can assume that the negative dynamics of SOC may also be associated with insufficient stabilization of carbon in organo-mineral complexes. In contrast, S10 retains higher SOC/clay (0.23–0.26) and SOC values (3.6–3.8%) due to continuous organic inputs and organo-clay complexes [13]. It was also found that the SOC content in the studied soils has a strong correlation with CEC (Pearson's r = 0.61, r^2 = 0.37). This correlation (Figure 7) may indicate that the content of exchangeable cations in the studied soils is mainly responsible for the organic matter rather than the mineral matrix of the soil; moreover, it was previously shown that the mineralogical composition here is extremely poor, with the dominance of quartz and the minimal presence of layered minerals (Figure 5).

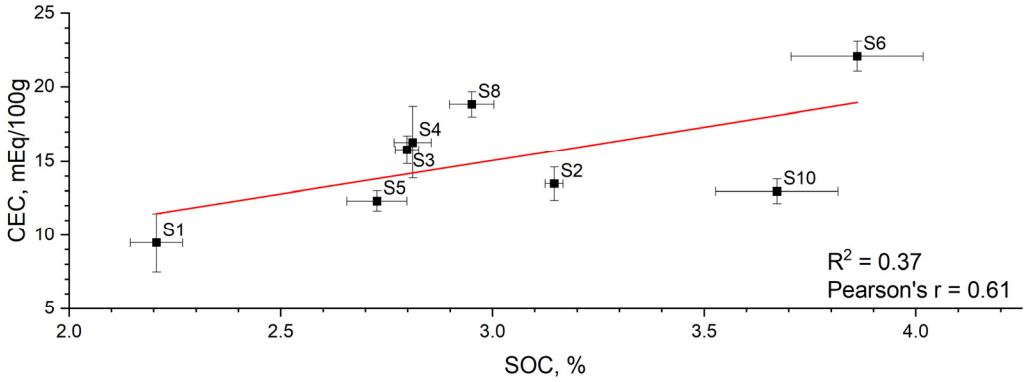

Figure 7. Scatter plot of SOC, % (mean ± SD, n = 3), and CEC, mEq/100 g (mean ± SD, n = 3), in a post-agrogenic soil chronosequence (S1–S8) and the Yamal experimental agrostation (S10).

In abandoned soil chronoseries, TN depletion is also observed [13], dropping by 39% (0.18% in S5 → 0.11% in S1), reflecting reduced fertilization and microbial nitrogen mining from SOM [75]. Bulk soil C:N ratios increased (Figure 8) from 19–20 (S5) to 22–30 (S1–S3), while the C:N ratio in SOM rose from 34 (S5) to 29–31 (S1), aligning with shifts toward lignin-rich, nitrogen-poor organic matter and mirroring boreal post-agrogenic systems [76–78]. The SOM C:N ratio (21–35) exceeded the bulk C:N ratio (17–26), highlighting preferential N retention in microbial biomass or mineral-associated SOM.

The van Krevelen diagram (Figure 9) shows that abandoned soils (e.g., S1: O:C = 0.82–0.83) show higher oxidation than active fields (S5: O:C = 0.68–0.69), suggesting advanced SOM decomposition. The reference site (S10: O:C = 0.66–0.67) has stable, less oxidized SOM. The rise in O:C ratios in abandoned soils (S1: 0.82–0.83) signals oxidative humification, a process intensified by prolonged exposure of SOM in poorly protected quartz matrices [79,80].

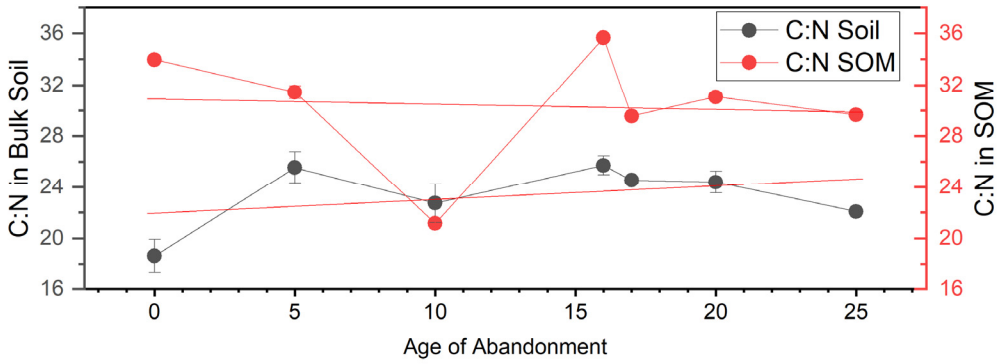

Figure 8. Variation in C:N ratios in bulk soil and in SOM (mean ± SD, n = 3) depending on the period of soil abandonment.

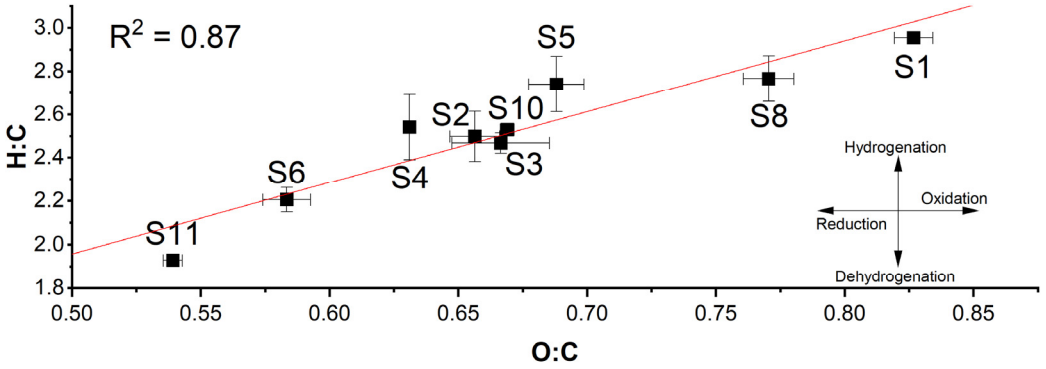

Figure 9. The van Krevelen diagram (O:C to H:C, mean ± SD (n = 3)) for SOM elemental analysis results.

^{13}C NMR analysis provides insights into molecular reorganization (Figures 10 and 11). Active fields (S5: alkyl C = 40.88%, A/O-A = 1.55) have more labile alkyl C, while older abandoned soils (S8: alkyl C = 31.65%, A/O-A = 1.13) show dominance of O-alkyl C (e.g., carbohydrates). The high alkyl C content also detected in an active field (S5—40.88%) reflects labile plant lipids, which decompose rapidly when tillage disrupts aggregates [81,82]. Reduced alkyl C (Figure 10) and HB/HI (Figure 11) values correlate with diminished physical protection, as hydrophobic alkyl moieties degrade under repeated freeze–thaw cycles [83,84]. This aligns with studies on Siberian permafrost soils, where SOM loss accelerated under warming [85]. The reference site (S10: 39.61% alkyl C) retains similar levels due to continuous organic inputs [86]. The proportion of O-alkyl C (60–110 ppm) gradually increases (20.6–21.6 %), despite a decrease in SOC concentration ($r = -0.41$, $p < 0.05$), indicating a transient input of plant-derived organic matter from fresh organic residues from the shrub litter. Dominance of O-alkyl C in abandoned soils indicates microbial processing into polysaccharides, which persist due to slower decomposition in cold climates [46]. This mirrors patterns where O-alkyl C accumulated in abandoned agricultural plots [87]. Increased aryl C in mid-abandonment (S8: 15.88%) reflects lignin accumulation, a recalcitrant pool resistant to cold-climate decomposition [88]. However, without mineral binding, aromatic SOM remains vulnerable to photodegradation [89].

We acknowledge that it is difficult to provide detailed knowledge of the stability of SOC pools in these soils without a comprehensive study of carbon, specifically in particulate and mineral-associated organic carbon (POC and MAOC) fractions, but our results allow us to provide indirect conclusions. Mineral-protected SOC in soils is primarily formed from organo-mineral interactions with secondary minerals by weathering over long periods, varying from decades to centuries, prohibiting the accumulation of a substantial amount of MAOC in a short time [90]. It is known that SOC in stable aggregates has a slower turnover

than free POM [91]. Our results show that minerals with low reactive capacity (quartz) are dominant in soils and parent materials, while layered minerals (vermiculite, etc.) are present in considerably lower quantities (Figure 5). In addition, we observed a strong correlation (r = 0.61) of SOC in bulk soil with CEC (Figure 7), indicating a significant contribution of past fertilization to increasing sorption capacity in soils with a poor mineralogical composition [92]. All other things being equal, there has been a substantial reorganization of the molecular structure of SOM, with oxidation (Figure 9), an increase in aromaticity, and a decrease in hydrophobicity over time (Figure 11). This may indicate a lack of physical protection of SOM, since at high degrees of occlusion, the organic matter is generally poorly accessible to microorganisms [43,90,93], but the data indicate that under these Subarctic conditions, the labile fraction of SOM is gradually replaced by coarse organic residues (O-alkyl C accumulation).

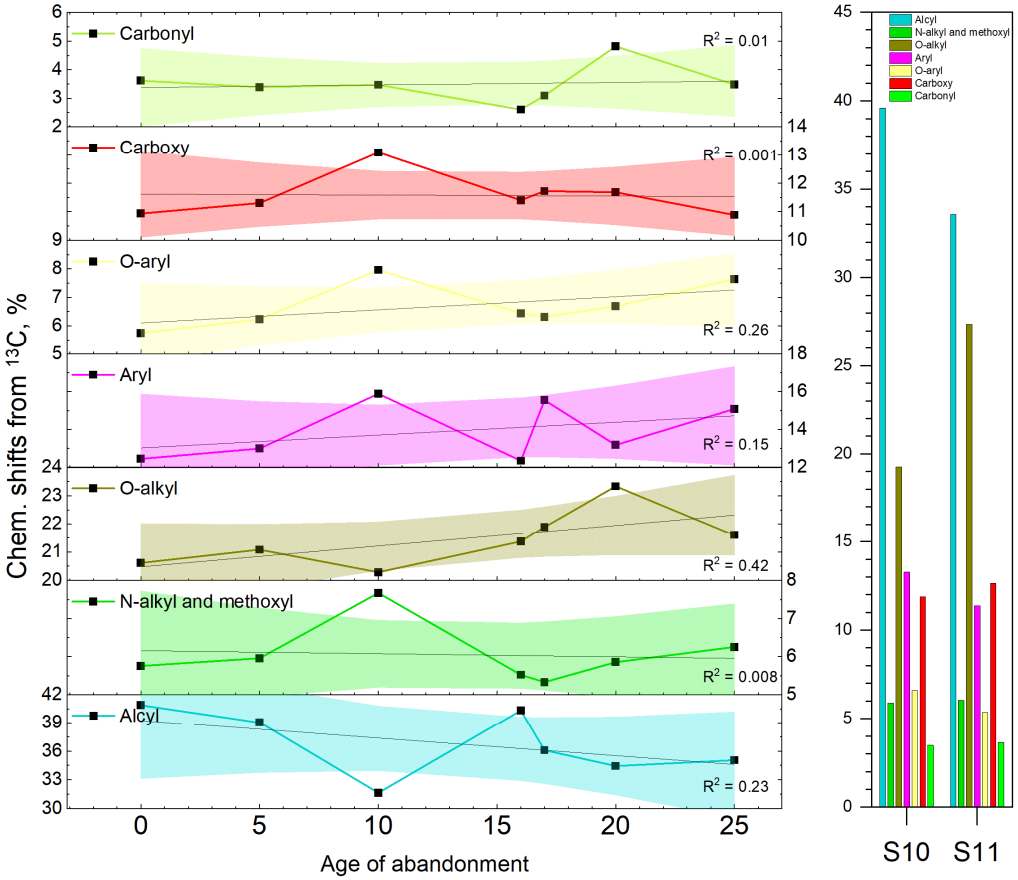

Figure 10. Dynamics of molecular structure in the soil chronosequence according to ^{13}C NMR. S10—molecular structure of SOM in soil of Yamal Agricultural Station, S11—molecular structure of SOM in reference peat soil.

There is a notion that repeated freezing and thawing disrupts soil aggregates, exposing physically protected SOM to microbial decomposition and oxidative processes [71,94]. In quartz-rich soils, the absence of clay minerals (e.g., vermiculite) exacerbates this vulnerability, as aggregates rely only on weak organic binding agents [95]. This aligns with the findings of those who observed accelerated SOM loss in mineral-poor Arctic soils subjected to freeze–thaw events [96].

Quartz, with negligible cation exchange capacity and surface reactivity, fails to stabilize SOM through organo-mineral associations [69]. This contrasts with temperate soils, where clays and oxides dominate SOM stabilization [65,97]. Long-term fertilization at S10 sustains SOC (3.58–3.83%) and stable alkyl C (A/O-A = 1.57). Fertilization through

high organic inputs compensates for slow nutrient cycling and supports microbial activity, stabilizing SOM through organo-mineral associations. Similar results were reported in Finnish cropland soils, where manure application maintained SOM in soils [98]. We can assume that changes in the structural composition and stabilization of SOM result from several processes illustrated in Figure 12 and described below.

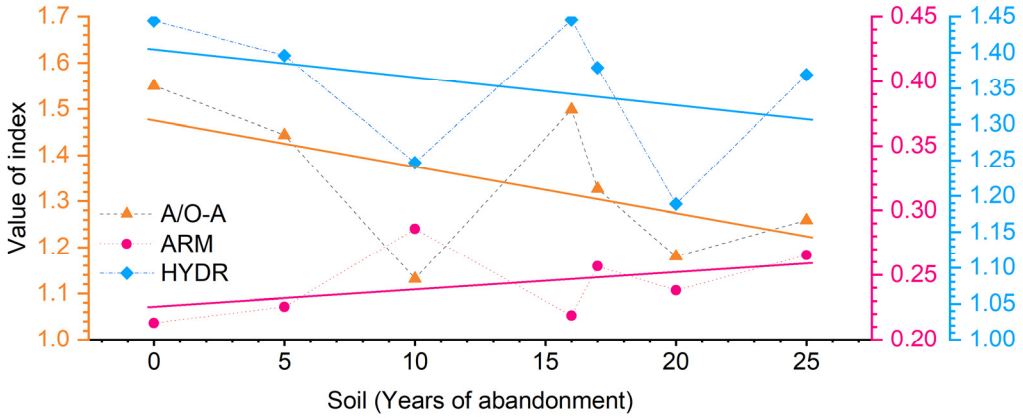

Figure 11. Integral indexes of SOM quality in soil chronosequence. ARM—aromaticity index HB/HI—hydrophobicity index, A/O-A—alkyl C/O-alkyl C.

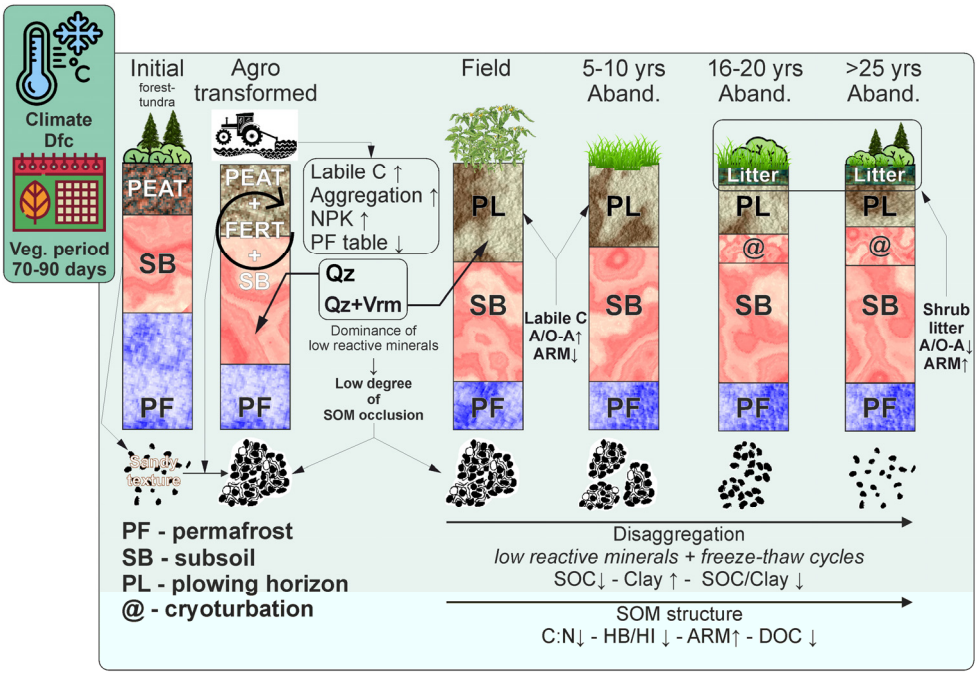

Figure 12. Visualization of processes in agro-transformed soils in Subarctic climatic conditions. 1—Primary involvement of mature soils in agriculture promotes saturation of soil with labile C and nutrients and stimulates aggregate formation. 2—Low temperatures and a short growing season inhibit humification of fresh plant residues, leading to lignin accumulation and an increase in aromaticity after abandonment. 3—Mineral matrix dominated by quartz does not allow occlusion processes and formation of a physically protected SOM pool, while freeze–thaw cycles contribute to disaggregation of earlier formed aggregates.

1—Cold temperatures reduce decomposition rates but favor selective preservation of complex compounds [99,100]. 2—Freeze–thaw cycles disrupt soil structure, accelerating SOM oxidation [101]. 3—Short growing seasons limit plant-derived C inputs, exacerbating SOM decline in unmanaged systems [97]. These assumptions are indirectly supported by

the results of the PCA analysis (Table 4). PC1 (35.5% of variance)—associated with DOC, C:N, P, K, and NH_4—reflects the processes of continuous active soil management, which in combination with the poor mineralogical composition of soils and freeze–thaw cycles does not allow long-term retention of nutrients, and short growing seasons do not allow the accumulation and recycling of fresh organic residues. The PC1 gradient (Figure 4) separates the active/reference soils (S5 and S10) from older abandoned soils. High P/K and labile C indicate sustained fertility from fertilization, counteracting Subarctic nutrient limitations. PC2 (25.9% of variance)—related to SOC, NO_3, and SOM characteristics (O:C, H:C, A/O-A, HB/HI, and ARM)—reflects decomposition and stabilization of organic matter, while cold temperatures slowed decomposition but failed to offset SOC losses in abandoned soils due to limited inputs. The PC2 gradient (Figure 4) also separates the active/reference soils from older abandoned soils and decreases predominantly for young abandoned soils with older abandoned soils, indicating disrupted SOM stability in abandoned soils. PC3 (18.1% of variance) is related to pH, P, and the C:N ratio; also, PC3 has the highest loading for clay content (0.35). This PC likely reflects the increased capacity of soils to sorb P at a high SOM content and a high SOM humification rate, as indicated by high opposite loadings for P and SOM C:N ratios (Table 4). Previously, similar results were reported for fertilized sandy soils at different pH gradients [95].

5. Conclusions

This study justifies the complex interplay of climatic, mineralogical, and anthropogenic factors with respect to SOM dynamics in Subarctic agricultural soils. The chronosequence analysis revealed that short-term abandonment (5–10 years) initially enhances SOC due to reduced tillage and plant-residue accumulation. However, prolonged abandonment (>20 years) leads to significant SOC depletion (2.15–2.27%), driven by oxidative humification and mineralization in quartz-dominated soils with imperceptible organo-mineral stabilization. The absence of reactive clay minerals (e.g., vermiculite) and the dominance of quartz—a mineral with a low cation exchange capacity—render SOM reliant on physical occlusion and biochemical recalcitrance, both of which are vulnerable to Subarctic freeze–thaw cycles that disrupt aggregates. ^{13}C NMR spectroscopy provided critical insights into molecular shifts: active fields exhibited labile alkyl-C (40.88%), indicative of fresh plant inputs, while abandoned soils showed progressive enrichment of O-alkyl-C (21.6%) and aryl-C (15.88%), signaling microbial processing and lignin accumulation. Despite lignin's recalcitrance, its vulnerability to degradation in mineral-poor matrices underscores the instability of SOM in unmanaged systems. In contrast, the reference site of the Yamal experimental agrostation (S10) demonstrated resilience through continuous organic fertilization, maintaining alkyl-C (39.61%) and moderate aromaticity (ARM = 0.23). This stability arises from organo-mineral interactions with limited clay minerals, highlighting the role of sustained organic inputs in bypassing mineralogical constraints.

Key climatic stressors—short growing seasons and freeze–thaw cycles—amplify SOM degradation. Cold temperatures slow microbial decomposition but fail to offset SOC losses due to limited fresh C inputs in abandoned soils. PCA analysis further linked SOC decline to nutrient leaching (P and K) and acidification, which inhibit microbial activity. The rise in O:C ratios (0.68 to 0.83) and declining hydrophobicity (HB/HI = 1.44 to 1.19) in abandoned soils validate advanced oxidation and loss of alkyl compounds. Sustainable management must prioritize organic amendments (e.g., peat and manure) to enhance SOC retention, as evidenced by the reference site's success. However, pure peat applications risk oxidation unless integrated with mineral soils.

For a more detailed investigation of the post-agrogenic transformation processes of SOM in soils of the Subarctic, it is essential to continue studies on its structure through

deeper fractionation of SOM—separation of the total SOM pool into Particulate Organic Matter (POM) and Mineral-Associated Organic Matter (MAOM), in conjunction with the analysis of the mineral composition of the clay fractions of these soils. In the long term, this approach will allow for the identification of the peculiarities of organo-mineral interactions under the harsh conditions of the Arctic.

Subarctic agricultural abandonment raises significant risks to SOM persistence, which requires proactive management strategies to mitigate carbon loss. Long-term fertilization emerges as a viable approach to sustain soil health, emphasizing the need for policies that support organic input regimes in Arctic agriculture. This work contributes to global understanding of SOM dynamics in cold climates, offering critical insights for carbon management in the face of rapid Arctic warming.

Author Contributions: Conceptualization, T.N. and E.A.; methodology, E.A. and S.Y.; software, T.N.; validation, S.Y. and X.W.; formal analysis, E.A. and S.Y.; investigation, E.A., V.G. and T.N.; resources, E.A. and S.Y.; data curation, T.N. and V.G.; writing—original draft preparation, T.N.; writing—review and editing, E.A. and V.G.; visualization, T.N.; supervision, E.A. and S.Y.; project administration, E.A.; funding acquisition, E.A. and S.Y. All authors have read and agreed to the published version of the manuscript.

Funding: For T.N. and E.A., research was funded by the Russian Science Foundation (Grant No. 24-44-00006); for S.Y. and X.W., research was funded by the National Natural Science Foundation of China (Grant No. 32361133551).

Data Availability Statement: Data can be obtained upon request from the corresponding author. The data are not publicly available due to privacy.

Acknowledgments: The authors are grateful to the Department of External Relations of the Yamal–Nenets Autonomous District and to the Arctic Research Center of the Yamal–Nenets Autonomous District for assistance in conducting and organizing the fieldwork. The authors thank the Research Park of St. Petersburg State University (the Research Center of Chemical Analyses, the Centre for X-ray Diffraction Studies and Materials Research, and the Magnetic Resonance Research Center).

Conflicts of Interest: The authors declare no conflicts of interest.

Abbreviations

The following abbreviations are used in this manuscript:

SOM	Soil Organic Matter
SOC	Soil Organic Carbon
TN	Total Nitrogen
CEC	Cation Exchange Capacity
NMR	Nuclear Magnetic Resonance
PXRD	Powder X-Ray Diffraction
YAS	Yamal Experimental Agricultural Station
MT	Mature Soil
ARM	Aromaticity index
HB/HI	Hydrophobicity index
DOC	Dissolved Organic Compounds in SOC
PCA	Principal Component Analysis
CV	Coefficient of Variation

Appendix A

Table A1. Bulk soil parameters used in this paper, obtained previously (S5–S1) [31]. Characteristics of bulk soil of Yamal experimental agricultural station (S10), obtained by methods similar to those described in the article [31]. BD—bulk density, SOC—soil organic carbon, TN—total nitrogen, P—mobile phosphorous, K—mobile potassium, N-NH_4—ammonia nitrogen, N-NO_3—nitrate nitrogen (means ± SDs).

Soil	BD	Clay	pH	SOC	TN	C:N	P	K	N-NH_4	N-NO_3
Units	g cm^{-3}	%	-	%	%	-	mg kg^{-1}	mg kg^{-1}	mg kg^{-1}	mg kg^{-1}
S5	1.07	5.26 ± 0.26	4.4 ± 0.2	2.73 ± 0.07	0.17 ± 0.01	18.63 ± 1.28	1115.67 ± 22.94	1145.33 ± 20.13	302.41 ± 19.95	16.70 ± 2.01
S6	1.20	7.53 ± 0.20	4.3 ± 0.2	3.86 ± 0.16	0.18 ± 0.01	25.54 ± 1.23	322.67 ± 6.81	43.67 ± 1.53	15.92 ± 9.26	12.54 ± 3.02
S8	1.12	7.00 ± 0.35	5.3 ± 0.1	2.95 ± 0.05	0.15 ± 0.01	22.74 ± 1.50	944.33 ± 32.01	55.33 ± 5.03	9.01 ± 0.56	0.61 ± 0.21
S4	1.18	7.81 ± 0.46	4.5 ± 0.5	2.81 ± 0.04	0.13 ± 0.01	25.71 ± 0.74	248.00 ± 25.94	37.00 ± 5.20	12.85 ± 0.99	0.81 ± 0.25
S2	1.12	10.38 ± 0.34	4.0 ± 0.2	3.15 ± 0.02	0.15 ± 0.01	24.55 ± 0.19	365.67 ± 16.26	40.67 ± 2.52	12.50 ± 0.53	1.42 ± 0.31
S3	0.98	10.70 ± 0.60	4.2 ± 0.1	2.80 ± 0.03	0.13 ± 0.01	24.40 ± 0.86	409.00 ± 6.24	46.67 ± 14.50	17.39 ± 0.75	0.28 ± 0.07
S1	1.29	12.46 ± 0.88	4.1 ± 0.1	2.21 ± 0.06	0.12 ± 0.01	22.09 ± 0.18	215.33 ± 11.50	50.67 ± 6.51	14.31 ± 0.43	1.05 ± 0.61
S10	1.25	14.80 ± 1.03	4.8 ± 0.3	3.67 ± 0.14	0.22 ± 0.01	19.78 ± 0.79	977.33 ± 29.87	80.33 ± 9.07	13.62 ± 0.63	32.32 ± 1.78

References

1. Joshi, R.K.; Garkoti, S.C.; Gupta, R.; Kumar, S.; Mishra, A.; Kumar, M. Recovery of soil microbial biomass, stoichiometry, and herb-layer diversity with chronosequence of farmland land abandonment in the central Himalayas, India. *Restor. Ecol.* **2023**, *31*, e13782.
2. Levers, C.; Schneider, M.; Prishchepov, A.V.; Estel, S.; Kuemmerle, T. Spatial variation in determinants of agricultural land abandonment in Europe. *Sci. Total Environ.* **2018**, *644*, 95–111. [PubMed]
3. Zhou, J.; Sun, T.; Shi, L.; Kurganova, I.; de Gerenyu, V.L.; Kalinina, O.; Giani, L.; Kuzyakov, Y. Organic carbon accumulation and microbial activities in arable soils after abandonment: A chronosequence study. *Geoderma* **2023**, *435*, 116496.
4. Kalinina, O.; Cherkinsky, A.; Chertov, O.; Goryachkin, S.; Kurganova, I.; de Gerenyu, V.L.; Lyuri, D.; Kuzyakov, Y.; Giani, L. Post-agricultural restoration: Implications for dynamics of soil organic matter pools. *Catena* **2019**, *181*, 104096. [CrossRef]
5. Cramer, V.A.; Hobbs, R.J.; Standish, R.J. What's new about old fields? Land abandonment and ecosystem assembly. *Trends Ecol. Evol.* **2008**, *23*, 104–112.
6. Yang, Y.; Hobbie, S.E.; Hernandez, R.R.; Fargione, J.; Grodsky, S.M.; Tilman, D.Y.; Zhu, G.; Luo, Y.; Smith, T.M.; Jungers, J.M.; et al. Restoring abandoned farmland to mitigate climate change on a full earth. *One Earth* **2020**, *3*, 176–186.
7. Żarczyński, P.J.; Krzebietke, S.J.; Sienkiewicz, S.; Wierzbowska, J. The Role of Fallows in Sustainable Development. *Agriculture* **2023**, *13*, 2174. [CrossRef]
8. Kozak, M.; Pudełko, R. Impact Assessment of the Long-Term Fallowed Land on Agricultural Soils and the Possibility of Their Return to Agriculture. *Agriculture* **2021**, *11*, 148. [CrossRef]
9. Lasanta, T.; Arnáez, J.; Pascual, N.; Ruiz-Flaño, P.; Errea, M.P.; Lana-Renault, N. Space–time process and drivers of land abandonment in Europe. *Catena* **2017**, *149*, 810–823.
10. Beillouin, D.; Corbeels, M.; Demenois, J.; Berre, D.; Boyer, A.; Fallot, A.; Feder, F.; Cardinael, R. A global meta-analysis of soil organic carbon in the Anthropocene. *Nat. Commun.* **2023**, *14*, 3700.
11. Poeplau, C.; Don, A. Carbon sequestration in agricultural soils via cultivation of cover crops—A meta-analysis. *Agric. Ecosyst. Environ.* **2015**, *200*, 33–41.
12. Qin, W.; Wang, K.; Min, K.; Zhang, Y.; Wang, Z.; Liu, X. Agricultural land abandonment promotes soil aggregation and aggregate-associated organic carbon accumulation: A global meta-analysis. *Plant Soil* **2024**, *503*, 629–644.
13. Nizamutdinov, T.; Yang, S.; Abakumov, E. Post-Agricultural Shifts in Soils of Subarctic Environment on the Example of Plaggic Podzols Chronosequence. *Agronomy* **2025**, *15*, 584. [CrossRef]
14. Abakumov, E.; Morgun, E.; Pechkin, A.; Polyakov, V. Abandoned agricultural soils from the central part of the Yamal region of Russia: Morphology, diversity, and chemical properties. *Open Agric.* **2020**, *5*, 94–106.
15. Desyatkin, A.R.; Iwasaki, S.; Desyatkin, R.V.; Hatano, R. Changes of Soil C Stock under Establishment and Abandonment of Arable Lands in Permafrost Area—Central Yakutia. *Atmosphere* **2018**, *9*, 308. [CrossRef]
16. Deng, L.; Zhu, G.; Tang, Z.; Shangguan, Z. Global patterns of the effects of land-use changes on soil carbon stocks. *Glob. Ecol. Conserv.* **2016**, *5*, 127–138.
17. Xiong, X.; Grunwald, S.; Myers, D.B.; Ross, C.W.; Harris, W.G.; Comerford, N.B. Interaction effects of climate and land use/land cover change on soil organic carbon sequestration. *Sci. Total Environ.* **2014**, *493*, 974–982.
18. Davidson, E.A.; Janssens, I.A. Temperature Sensitivity of Soil Carbon Decomposition and Feedbacks to Climate Change. *Nature* **2006**, *440*, 165–173.

19. Rodrigues, C.I.D.; Brito, L.M.; Nunes, L.J.R. Soil Carbon Sequestration in the Context of Climate Change Mitigation: A Review. *Soil Syst.* **2023**, *7*, 64. [CrossRef]
20. Hoffland, E.; Kuyper, T.W.; Comans, R.N.J.; Creamer, R.E. Eco-functionality of organic matter in soils. *Plant Soil* **2020**, *455*, 1–22.
21. Li, J.; Ramires, G.H.; Kiani, M.; Quideau, S.; Smith, E.; Janzen, H.; Larney, F.; Puurveen, D. Soil organic matter dynamics in long-term temperate agroecosystems: Rotation and nutrient addition effects. *Can. J. Soil Sci.* **2018**, *98*, 232–245.
22. Lal, R. Soil carbon sequestration impacts on global climate change and food security. *Science* **2004**, *304*, 1623–1627.
23. Schmidt, M.W.I.; Torn, M.S.; Abiven, S.; Dittmar, T.; Guggenberger, G.; Janssens, I.A.; Kleber, M.; Kögel-Knabner, I.; Lehmann, J.; Manning, D.A.C. Persistence of soil organic matter as an ecosystem property. *Nature* **2011**, *478*, 49–56.
24. White, D.M.; Garland, D.S.; Ping, C.L.; Michaelson, G. Characterizing soil organic matter quality in arctic soil by cover type and depth. Cold Reg. *Sci. Technol.* **2004**, *38*, 63–73.
25. Nizamutdinov, T.; Zhemchueva, D.; Zverev, A.; Andronov, E.; Pechkin, A.; Abakumov, E. Agropedogenesis and related changes in morphology, fertility and microbiome diversity of soils in cryogenic ecosystems on the example of the central part of Yamal region (West Siberia). *Geoderma* **2024**, *449*, 117014.
26. Mosa, A.A.; Taha, A.; Elsaeid, M. Agro-environmental applications of humic substances: A critical review. *Egypt. J. Soil Sci.* **2020**, *60*, 207–220.
27. Hugelius, G.; Strauss, J.; Zubrzycki, S.; Harden, J.W.; Schuur, E.A.; Ping, C.-L.; Schirrmeister, L.; Grosse, G.; Michaelson, G.J.; Koven, C.D. Estimated stocks of circumpolar permafrost carbon with quantified uncertainty ranges and identified data gaps. *Biogeosciences* **2014**, *11*, 6573–6593.
28. Unc, A.; Altdorff, D.; Abakumov, E.; Adl, S.; Baldursson, S.; Bechtold, M.; Cattani, D.J.; Firbank, L.G.; Grand, S.; Guðjónsdóttir, M.; et al. Expansion of Agriculture in Northern Cold-Climate Regions: A Cross-Sectoral Perspective on Opportunities and Challenges. *Front. Sustain. Food Syst.* **2021**, *5*, 663448.
29. Altdorff, D.; Borchard, N.; Young, E.H.; Galagedara, L.; Sorvali, J.; Quideau, S.; Unc, A. Agriculture in boreal and Arctic regions requires an integrated global approach for research and policy. *Agron. Sustain. Dev.* **2021**, *41*, 23.
30. Poeplau, C.; Schroeder, J.; Gregorich, E.; Kurganova, I. Farmers' Perspective on Agriculture and Environmental Change in the Circumpolar North of Europe and America. *Land* **2019**, *8*, 190. [CrossRef]
31. Schroeder, J.; Peplau, T.; Pennekamp, F.; Gregorich, E.; Tebbe, C.C.; Poeplau, C. Deforestation for agriculture increases microbial carbon use efficiency in subarctic soils. *Biol. Fertil. Soils* **2024**, *60*, 17–34. [CrossRef]
32. Alekseeva, L.V. The Formation of Polar Agriculture in the USSR (Based on the Materials of Yamal). *Bull. Nizhnevartovsk State Univ.* **2017**, *2*, 3–10. (In Russian)
33. Nizamutdinov, T.; Abakumov, E.; Morgun, E.; Loktev, R.; Kolesnikov, R. Agrochemical and Pollution Status of Urbanized Agricultural Soils in the Central Part of Yamal Region. *Energies* **2021**, *14*, 4080. [CrossRef]
34. Doetterl, S.; Berhe, A.A.; Heckman, K.; Lawrence, C.; Schnecker, J.; Vargas, R.; Vogel, C.; Wagai, R. A landscape-scale view of soil organic matter dynamics. *Nat. Rev. Earth Environ.* **2025**, *6*, 67–81. [CrossRef]
35. Nizamutdinov, T.I.; Suleymanov, A.R.; Morgun, E.N.; Dinkelaker, N.V.; Abakumov, E.V. Ecotoxicological analysis of fallow soils at the Yamal experimental agricultural station. *Food Process. Tech. Technol.* **2022**, *52*, 350–360. [CrossRef]
36. Herndon, E.M.; Yang, Z.; Bargar, J.; Janot, N.; Regier, T.Z.; Graham, D.E.; Liang, L. Geochemical drivers of organic matter decomposition in arctic tundra soils. *Biogeochemistry* **2015**, *126*, 397–414. [CrossRef]
37. Abakumov, E.; Zverev, A.; Morgun, E.; Alekseev, I. Microbiome of Abandoned Agricultural and Mature Tundra Soils in Southern Yamal Region. Russian Arctic. *Open Agric.* **2020**, *5*, 335–344. [CrossRef]
38. Jastrow, J.D.; Miller, R.M. Soil aggregate stabilisation and carbon sequestration: Feedbacks through organomineral associations. In *Soil Processes and the Carbon Cycle*; Lal, R., Kimble, J.M., Follett, R.F., Stewart, B.A., Eds.; CRC Press: Boca Raton, FL, USA, 1997; pp. 207–223.
39. Dignac, M.-F.; Derrien, D.; Barre, P.; Barot, S.; Cécillon, L.; Chenu, C.; Chevallier, T.; Freschet, G.T.; Garnier, P.; Guenet, B.; et al. Increasing soil carbon storage: Mechanisms, effects of agricultural practices and proxies. A review. *Agron. Sustain. Dev.* **2017**, *37*, 14. [CrossRef]
40. Ondrasek, G.; Begic, H.B.; Zovko, M.; Filipović, L.; Meriño-Gergichevich, C.; Savić, R.; Rengel, Z. Biogeochemistry of soil organic matter in agroecosystems & environmental implications. *Sci. Total Environ.* **2019**, *658*, 1559–1573.
41. Crews, T.E.; Rumsey, B.E. What Agriculture Can Learn from Native Ecosystems in Building Soil Organic Matter: A Review. *Sustainability* **2017**, *9*, 578. [CrossRef]
42. Semenov, V.M.; Tulina, A.S.; Semenova, N.A.; Ivannikova, L.A. Humification and nonhumification pathways of the organic matter stabilization in soil: A review. *Eurasian Soil Sci.* **2013**, *46*, 355–368. [CrossRef]
43. Lützow, M.; Kögel-Knabner, I.; Ekschmitt, K.; Matzner, E.; Guggenberger, G.; Marschner, B.; Flessa, H. Stabilization of organic matter in temperate soils: Mechanisms and their relevance under different soil conditions—A review. *Eur. J. Soil Sci.* **2006**, *57*, 426–445. [CrossRef]

44. Haddaway, N.R.; Hedlund, K.; Jackson, L.E.; Kätterer, T.; Lugato, E.; Thomsen, I.K.; Jørgensen, H.B.; Isberg, P.-E. How does tillage intensity affect soil organic carbon? A systematic review. *Environ. Evid.* **2017**, *6*, 30.
45. Lodygin, E.; Abakumov, E. The Use of Spectroscopic Methods to Study Organic Matter in Virgin and Arable Soils: A Scoping Review. *Agronomy* **2024**, *14*, 1003. [CrossRef]
46. Baldock, J.A.; Oades, J.M.; Nelson, P.N.; Skene, T.M.; Golchin, A.; Clarke, P. Assessing the extent of decomposition of natural organic materials using solid-state ^{13}C NMR spectroscopy. *Aust. J. Soil Res.* **1997**, *35*, 1061–1083. [CrossRef]
47. Audette, Y.; Congreves, K.A.; Schneider, K.; Zaro, G.C.; Nunes, A.L.P.; Zhang, H.; Voroney, R.P. The effect of agroecosystem management on the distribution of C functional groups in soil organic matter: A review. *Biol. Fertil. Soils* **2021**, *57*, 881–894. [PubMed]
48. Chukov, S.N.; Lodygin, E.D.; Abakumov, E.V. Application of ^{13}C NMR spectroscopy to the study of soil organic matter: A review of publications. *Eurasian Soil Sci.* **2018**, *51*, 889–900.
49. Kögel-Knabner, I.; Guggenberger, G.; Kleber, M.; Kandeler, E.; Kalbitz, K.; Scheu, S.; Eusterhues, K.; Leinweber, P. Organo-mineral associations in temperate soils: Integrating biology, mineralogy, and organic matter chemistry. *J. Plant Nutr. Soil Sci.* **2008**, *171*, 61–82.
50. Suleymanov, A.; Nizamutdinov, T.; Morgun, E.; Abakumov, E. Evaluation and Spatial Variability of Cryogenic Soil Properties (Yamal-Nenets Autonomous District, Russia). *Soil Syst.* **2022**, *6*, 65. [CrossRef]
51. Tikhanovsky, A.N. Potatoes in Yamal. In *Novosibirsk*; Publishing House "Akademizdat": Moscow, Russia, 2021; 160p. (In Russian)
52. IUSS Working Group WRB. *World Reference Base for Soil Resources. International Soil Classification System for Naming Soils and Creating Legends for Soil Maps*, 4th ed.; IUSS: Vienna, Austria, 2022.
53. Bahadori, M.; Chen, C.; Lewis, S.; Boyd, S.; Rashti, M.R.; Esfandbod, M.; Garzon-Garcia, A.; Van Zwieten, L.; Kuzyakov, Y. Soil organic matter formation is controlled by the chemistry and bioavailability of organic carbon inputs across different land uses. *Sci. Total Environ.* **2021**, *770*, 145307.
54. Mathers, N.J.; Xu, Z.H.; Berners-Price, S.J.; Perera, S.; Saffigna, P.G. Hydrofluoric acid pre-treatment for improving 13C CPMAS NMR spectral quality of forest soils in southeast Queensland, Australia. *Aust. J. Soil Res.* **2002**, *40*, 655–674.
55. Pizzanelli, S.; Calucci, L.; Forte, C.; Borsacchi, S. Studies of Organic Matter in Composting, Vermicomposting, and Anaerobic Digestion by ^{13}C Solid-State NMR Spectroscopy. *Appl. Sci.* **2023**, *13*, 2900. [CrossRef]
56. Vanchikova, E.V.; Shamrikova, E.V.; Sytar, T.S.; Kazakov, V.G. A new method to determine the carbon content of water-soluble organic compounds in soils. *Eurasian Soil Sci.* **2006**, *39*, 1084–1088.
57. FAO. *Standard Operating Procedure for Soil Organic Carbon. Walkley-Black Method: Titration and Colorimetric Method*; FAO: Rome, Italy, 2019.
58. Maskalchuk, L.N.; Baklai, A.A.; Leont'eva, T.G.; Makovskaya, N.A. Removal of Cesium Radionuclides from Aqueous Media with an Aluminosilicate Sorbent Prepared from Belaruskalii Production Waste. *Radiochemistry* **2019**, *61*, 459–463.
59. Elemile, O.O.; Ibitogbe, E.M.; Folorunso, O.P.; Ejiboye, P.O.; Adewumi, J.R. Principal component analysis of groundwater sources pollution in Omu-Aran community, Nigeria. Environmental Sciences, 80:690. *Environ. Earth Sci.* **2021**, *80*, 16.
60. Faloye, O.T.; Ajayi, A.E.; Kamchoom, V.; Akintola, O.A.; Oguntunde, P.G. Evaluating Impacts of Biochar and Inorganic Fertilizer Applications on Soil Quality and Maize Yield Using Principal Component Analysis. *Agronomy* **2024**, *14*, 1761. [CrossRef]
61. Lodygin, E.; Beznosikov, V.; Abakumov, E. Humic substances elemental composition of selected taiga and tundra soils from Russian European North-East. *Pol. Polar Res.* **2017**, *38*, 125–147. [CrossRef]
62. Nadal-Romero, E.; Rubio, P.; Kremyda, V.; Absalah, S.; Cammeraat, E.; Jansen, B.; Lasanta, T. Effects of agricultural land abandonment on soil organic carbon stocks and composition of soil organic matter in the Central Spanish Pyrenees. *Catena* **2021**, *205*, 105441.
63. Raiesi, F. Soil properties and C dynamics in abandoned and cultivated farmlands in a semi-arid ecosystem. *Plant Soil* **2012**, *351*, 161–175. [CrossRef]
64. Filimonenko, E.; Kurganova, I.; Uporova, M.; de Gerenyu, V.L.; Sokolova, L.; Zorina, S.; Dorofeev, N.; Maltseva, A.; Soldatova, E.; Gershelis, E.; et al. Energy storage and stability of soil organic matter during the natural restoration of abandoned cropland. *Agric. Ecosyst. Environ.* **2024**, *375*, 109198.
65. Balesdent, J.; Chenu, C.; Balabane, M. Relationship of soil organic matter dynamics to physical protection and tillage. *Soil Tillage Res.* **2000**, *53*, 215–230. [CrossRef]
66. Amelung, W.; Zech, W.; Flach, K. Climatic effects on soil organic matter composition in the Great Plains. *Soil Sci. Soc. Am. J.* **1997**, *61*, 115–123. [CrossRef]
67. Mani, S.; Merino, A.; García-Oliva, F.; Riotte, J.; Sukumar, R. Soil properties and organic matter quality in relation to climate and vegetation in southern Indian tropical ecosystems. *Soil Res.* **2018**, *56*, 80–90. [CrossRef]
68. Wasner, D.; Abramoff, R.; Griepentrog, M.; Venegas, E.Z.; Boeckx, P.; Doetterl, S. The role of climate, mineralogy and stable aggregates. *Glob. Biogeochem. Cycles* **2024**, *38*, e2023GB007934. [CrossRef]

69. Kleber, M.; Bourg, I.C.; Coward, E.K.; Hansel, C.M.; Myneni, S.C.; Nunan, N. Dynamic interactions at the mineral–organic matter interface. *Nat. Rev. Earth Environ.* **2021**, *2*, 402–421. [CrossRef]
70. Liang, C.; Schimel, J.P.; Jastrow, J.D. The importance of anabolism in microbial control over soil carbon storage. *Nat. Microbiol.* **2017**, *2*, 17105. [CrossRef]
71. Basile-Doelsch, I.; Balesdent, J.; Pellerin, S. Reviews and syntheses: The mechanisms underlying carbon storage in soil. *Biogeosciences* **2020**, *17*, 5223–5242. [CrossRef]
72. Six, J.; Bossuyt, H.; Degryze, S.; Denef, K. A history of research on the link between (micro) aggregates, soil biota, and soil organic matter dynamics. *Soil Tillage Res.* **2004**, *79*, 7–31. [CrossRef]
73. Nadporozhskaya, M.A.; Bykhovets, S.S.; Nizamutdinov, T.I.; Morgun, E.N.; Abakumov, E.V. Analysis of organic matter stock dynamics in arable soils of Yamal: Simulation experiments with the ROMUL model. *Dokuchaev Soil Bull.* **2024**, *120*, 48–83. [CrossRef]
74. Singh, M.; Sarkar, B.; Sarkar, S.; Churchman, J.; Bolan, N.; Mandal, S.; Menon, M.; Purakayastha, T.J.; Beerling, D.J. Stabilization of Soil Organic Carbon as Influenced by Clay Mineralogy. In *Advances in Agronomy*; Elsevier: Amsterdam, The Netherlands, 2018; Volume 148, pp. 33–84. ISBN 978-0-12-815179-2.
75. Li, H.; Parent, L.E.; Karam, A.; Tremblay, C. Potential of sphagnum peat for improving soil organic matter, water holding capacity, bulk density and potato yield in a sandy soil. *Plant Soil* **2004**, *265*, 355–365. [CrossRef]
76. Szajdak, L.W.; Jezierski, A.; Wegner, K.; Meysner, T.; Szczepański, M. Influence of Drainage on Peat Organic Matter: Implications for Development, Stability, and Transformation. *Molecules* **2020**, *25*, 2587. [CrossRef] [PubMed]
77. Ostrowska, A.; Porębska, G. Assessment of the C/N ratio as an indicator of the decomposability of organic matter in forest soils. *Ecol. Ind.* **2015**, *49*, 104–109.
78. van der Sloot, M.; Kleijn, D.; De Deyn, G.B.; Limpens, J. Carbon to nitrogen ratio and quantity of organic amendment interactively affect crop growth and soil mineral N retention. *Crop Environ.* **2022**, *1*, 161–167.
79. Lehmann, J.; Hansel, C.M.; Kaiser, C.; Kleber, M.; Maher, K.; Manzoni, S.; Nunan, N.; Reichstein, M.; Schimel, J.P.; Torn, M.S.; et al. Persistence of Soil Organic Carbon Caused by Functional Complexity. *Nat. Geosci.* **2020**, *13*, 529–534.
80. Yeasmin, S.; Singh, B.; Johnston, C.T.; Sparks, D.L. Organic carbon characteristics in density fractions of soils with contrasting mineralogies. *Geochim. Cosmochim. Acta* **2017**, *218*, 215–236.
81. Grandy, A.S.; Robertson, G.P. Land-use intensity effects on soil organic carbon accumulation rates and mechanisms. *Ecosystems* **2007**, *10*, 58–73.
82. Gupta, N.S.; Michels, R.; Briggs, D.E.; Collinson, M.E.; Evershed, R.P.; Pancost, R.D. Experimental evidence for the formation of geomacromolecules from plant leaf lipids. *Org. Geochem.* **2007**, *38*, 28–36.
83. Rumpel, C.; Seraphin, A.; Goebel, M.O.; Wiesenberg, G.; Gonzales--Vila, F.; Bachmann, J.; Schwark, L.; Michaelis, W.; Mariotti, A.; Kögel--Knabner, I. Alkyl C and hydrophobicity in B and C horizons of an acid forest soil. *J. Plant Nutr. Soil Sci.* **2004**, *167*, 685–692.
84. Höfle, S.; Rethemeyer, J.; Mueller, C.W.; John, S. Organic matter composition and stabilization in a polygonal tundra soil of the Lena Delta. *Biogeosciences* **2013**, *10*, 3145–3158.
85. Wild, B.; Gentsch, N.; Čapek, P.; Diáková, K.; Alves, R.J.E.; Bárta, J.; Gittel, A.; Hugelius, G.; Knoltsch, A.; Kuhry, P.; et al. Plant-derived compounds stimulate the decomposition of organic matter in arctic permafrost soils. *Sci. Rep.* **2016**, *6*, 25607.
86. Sonsri, K.; Mitsuboshi, M.; Watanabe, A. Stabilization mechanisms of organic matter in Andosols under long-term fertilization as revealed from structural, molecular, and stable isotopic signatures. *J. Soils Sediments* **2024**, *24*, 47–59.
87. Kurganova, I.; Merino, A.; Lopes de Gerenyu, V.O.; Barros, N.; Kalinina, O.; Giani, L.; Kuzyakov, Y. Mechanisms of carbon sequestration and stabilization by restoration of arable soils after abandonment: A chronosequence study on Phaeozems and Chernozems. *Geoderma* **2019**, *15*, 113882.
88. Grgas, D.; Rukavina, M.; Bešlo, D.; Štefanac, T.; Crnek, V.; Šikić, T.; Habuda-Stanić, M.; Landeka Dragičević, T. The Bacterial Degradation of Lignin—A Review. *Water* **2023**, *15*, 1272. [CrossRef]
89. Hussain, M.B.; Al-Hadidi, S.H.; Erfanian, M.B.; Yahia, M.N.D.; Mullungal, M.N.; Alsafran, M.; Bai, Y.; Alatalo, J.M. Photodegradation and Its Effect on Plant Litter Decomposition in Terrestrial Ecosystems: A Systematic Review. *Soil Syst.* **2023**, *7*, 6. [CrossRef]
90. Liu, M.; Zheng, S.; Pendall, E.; Smith, P.; Liu, J.; Li, J.; Fang, C.; Li, B.; Nie, M. Unprotected carbon dominates decadal soil carbon increase. *Nat. Commun.* **2025**, *16*, 2008. [PubMed]
91. Ozlu, E.; Arriaga, F.J. The role of carbon stabilization and minerals on soil aggregation in different ecosystems. *Catena* **2021**, *202*, 105303.
92. Nthebere, K.; Prakash, T.R.; Kumar, N.V.; Yadav, M.B.N. Capability of conservation agriculture for preservation of organic carbon and succeeding effect on soil properties and productivity-a review. *Arch. Agron. Soil Sci.* **2024**, *70*, 1–28.
93. Li, J.; Zhao, J.; Liao, X.; Hu, P.; Wang, W.; Ling, Q.; Xie, L.; Xiao, J.; Zhang, W.; Wang, K. Pathways of soil organic carbon accumulation are related to microbial life history strategies in fertilized agroecosystems. *Sci. Total Environ.* **2024**, *927*, 172191.

94. Matzner, E.; Borken, W. Do freeze-thaw events enhance C and N losses from soils of different ecosystems? A review. *Eur. J. Soil Sci.* **2008**, *59*, 274–284.
95. Debicka, M.; Kocowicz, A.; Weber, J.; Jamroz, E. Organic matter effects on phosphorus sorption in sandy soils. *Arch. Agron. Soil Sci.* **2016**, *62*, 840–855.
96. Hobbie, S.E.; Schimel, J.P.; Trumbore, S.E.; Randerson, J.R. Controls over Carbon Storage and Turnover in High-latitude Soils. *Glob. Change Biol.* **2000**, *6*, 196–210.
97. Sollins, P.; Kramer, M.G.; Swanston, C.; Lajtha, K.; Filley, T.; Aufdenkampe, A.K.; Wagai, R.; Bowden, R.D. Sequential density fractionation across soils of contrasting mineralogy: Evidence for both microbial- and mineral-controlled soil organic matter stabilization. *Biogeochemistry* **2009**, *96*, 209–231.
98. Heikkinen, J.; Ketoja, E.; Nuutinen, V.; Regina, K. Declining trend of carbon in Finnish cropland soils in 1974–2009. *Glob. Change Biol.* **2013**, *19*, 1456–1469.
99. Aerts, R. The freezer defrosting: Global warming and litter decomposition rates in cold biomes. *J. Ecol.* **2006**, *94*, 713–724.
100. Routh, J.; Hugelius, G.; Kuhry, P.; Filley, T.; Tillman, P.K.; Becher, M.; Crill, P. Multi-proxy study of soil organic matter dynamics in permafrost peat deposits reveal vulnerability to climate change in the European Russian Arctic. *Chem. Geol.* **2014**, *368*, 104–117.
101. Walz, J.; Knoblauch, C.; Böhme, L.; Pfeiffer, E. Regulation of soil organic matter decomposition in permafrost-affected Siberian tundra soils—Impact of oxygen availability, freezing and thawing, temperature, and labile organic matter. *Soil Biol. Biochem.* **2017**, *110*, 34–43.